Delft University of Technology

Bachelor Thesis

Applied Physics

Viscosity determination and attenuation measurements in non-Newtonian liquids using a ultrasonic waveguide

Author:
Koen Arends (4575148)

Supervisor:
Martin Rohde

To be defended on Wednesday 26th August 2020 at 10:00 AM.

Abstract

Conventional nuclear reactors can be a suitable solution to meet the increasing energy demand. However there is a lot of skepticism about the associated disadvantages, such as accessory radioactive waste and consequences of unsafe operation. Therefore a more safe and efficient type of nuclear reactor is investigated nowadays, which is the Molten Salt Reactor (MSR). The reason for these advantages is the fact that the reactor operates at high temperatures and atmospheric pressure. But since this reactor is relatively new and deals with salt mixtures as both fuel as well as a coolant it is important to know all properties at any time. Therefore one would like to monitor the properties such as density and viscosity constantly during performance. The latter is investigated in this research. The main research question is: 'How does the viscous behaviour and related attenuation by a powerlaw liquid (EAN) act for different high range frequencies of ultrasonic shear waves?'

In order to be able to measure in high temperature conditions a set up has been created which makes use of an ultrasonic waveguide. This setup is based on the research of Cegla et al[1] and Mastromarino et al[2]. Shear waves are sent through a plate, which is immersed into a fluid. After being reflected the waves are detected by a transducer. The attenuation of the signal strength caused by viscous dissipation is measured for different immersion depths of the plate into the fluid. For Newtonian fluids the attenuation is strongly related to the strength of the signal, which can be obtained by an exponential model. Besides, the viscosity can be calculated using the attenuation. For non-Newtonian fluids the attenuation and viscosity are also strongly related. This exponential dependence however does not hold anymore.

During the experiments on non-Newtonian fluids a powerlaw liquid named EAN (Ethyl Ammonium Nitrate) was used. For this liquid the attenuation of the signal was measured and another model to calculate the amplitude of the signal at different immersion depths by Rohde[3], based on the consistency (K) and the flow index (n), was tested. Using the data from Smith et al.[4], which already did some measurements on the rheology of EAN, values for these parameters of EAN were found, $n = 0.9822 \pm 0.006$ and $K = 35.47 \pm 1.05 Ns^n m^{-2}$. The value for K is accurate. However according to the model by Rohde a very small change in n gives a very big difference in corresponding amplitude of the signal. Due to the sensitivity for errors of n the obtained values for both K and n are not used. Therefore another way to investigate on EAN is examined.

In this research the ratio between the signal strengths at a fixed immersion depth for different frequencies is investigated instead for both water and EAN. The ratio is interesting since it does only depend on α for a fixed value of z. From this point the rheological behaviour of the fluid can be compared to water, since for water a theoretical model is found. For calculating the ratio a reference frequency of $3.0 MHz$ is used. For water the ratio follows exponential functions, where the lowest immersion depth gives the smallest change in ratio. For EAN a more parabolic trend is measured. The measurements however were very sensitive to measurement uncertainties. Some possible sources are the lack of cleaning the plate after each experiment, the sticking of the plate at the faces of the small container, and the failures of the LABVIEW program, which got stuck during some measurements. Also the level of the liquid inside the container as well as the amplitude of waves were not always constant during the measurements. These shortcomings and some small changes in the set up could cause

a lot of disturbance.

In future work, EAN or other salt mixtures should be further investigated. Some things which could help in making progress are using a larger container for EAN and a longer plate for the measurements for more accurate results. Experimentally the temperature dependency of EAN as well as the transmission by the transducer are important things to elaborate on. Besides that developing a rheological model for EAN is also strongly recommended.

Contents

Chapter 1: Introduction

The global energy consumption has been growing fastly the last years and our needs still ask for more and more. Nowadays the world energy consumption is 2-3% more than last year [5]. This is a worrying development, since the greatest part of the energy production is associated with lots of emitted CO2. In figure 1 is shown that approximately 80% of all supplied electricity in 2017 is produced by sources as coal and oil [6]. The main disadvantage of these products is that they are not renewable. Besides that, these fossil fuels are very harmful and dangerous in heating up the planet, because of the included emitted CO2. In order to provide ourselves with sufficient and sustainable energy in the future green energy could be an outcome, since it is more durable and cleaner. Some possible green options, such as wind energy, already occupy a certain part in our energy supply. Others are upcoming, such as biofuels, hydro energy and solar energy. Nuclear energy is another suitable alternative and already available from 1951 [7]. Despite the potential of nuclear energy many people are sceptical about the dependency on nuclear power after a few nuclear accidents in history, like in Chernobyl and Fukushima.

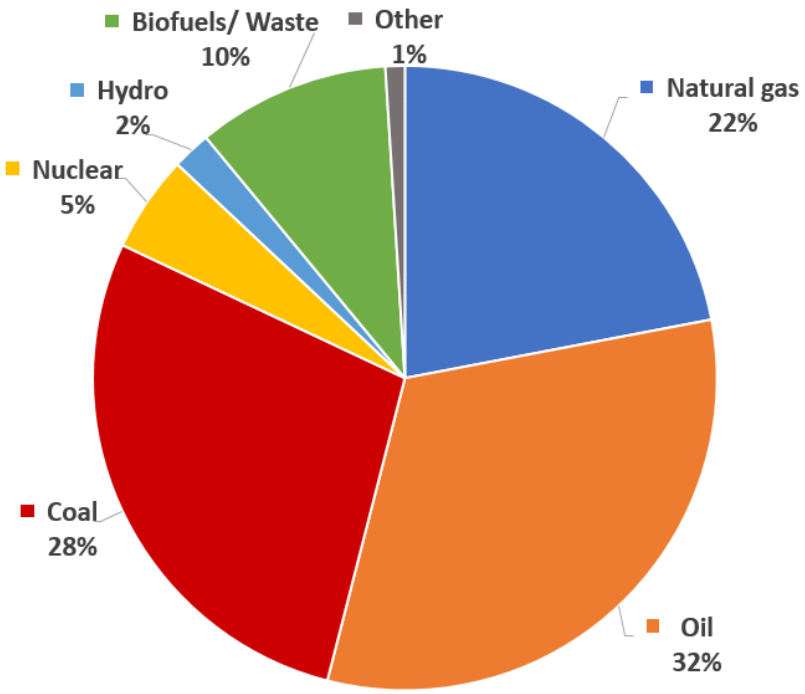

Figure 1: World energy production in 2017 [6]

Thermal neutron reactors, which is the most common type of nuclear reactor, produce energy by fission of uranium atoms. The biggest advantage of nuclear energy is the reliability compared to other types of 'CO2 neutral' energy, for instance solar energy. Besides that, a nuclear power plant produces large amounts of energy and the needed raw materials are relatively cheap and widely available. However, on the other side, the production of nuclear energy comes with fission products, which could be dangerous and cause disastrous consequences. Secondly, the production of nuclear energy includes radioactive waste. This waste has to be stored for a long time until it is not harmful anymore. For these reasons people are very careful in using nuclear energy at such a

large scale.

Nuclear reactors are optimized a lot over the years. Meanwhile there are four generations of nuclear reactors, from which only two generations are operational now. Most reactors, which produce electricity, are second generation reactors. Some are 3rd generation reactors. However it is necessary to meet the question, which arises nowadays, to provide ourselves a type of reactor which meets in covering the mentioned disadvantages, like the production of radioactive waste and dangerous fission products. Therefore the fourth generation reactors was designed and could be used to replace the contemporary reactors to be safer and more efficient in the future. These designs are made by the 'Generation IV International Forum (GIF)'. One of the criteria for this generation of reactors is the need to be highly economical. In addition, they must have enhanced safety, produce minimal waste and the system should be proliferation resistant [8]. The fourth generation reactors consist of six types of reactors, which are investigated all over the world. Some designs claim inherent safety, including the ability for more safety in loss of coolant scenarios. Others are designed to 'burn' waste from current reactors. On the drawing board this sounds very hopeful, although none has yet proven commercially viable. Three of the six designs are fast reactors and the other three are thermal reactors. Examples are the VHTR (very high temperature reactor), a supercritical water reactor and a lead-cooled fast reactor. Furthermore the molten salt reactor (MSR) also is one of the six types of fission reactors and is investigated at the TU Delft.

1.1 The MSR concept

The Molten Salt Reactor research started in the 1950s by Alvin Weinberg [9]. The first molten salt reactor experiments were conducted by Oak Ridge National Laboratory. At the moment the reactor is still in an experimental stage. The design was radical for its time and offered many advantages worth a fresh look today, since the molten salt mixture can be used both as fuel and as coolant in the reactor. This could make sure the reactor produces more efficiently, because a larger difference in temperature in a heat exchanger results in a higher Carnot thermal efficiency, and guarantees more safety. To accomplish this there is and will still be invested a lot on this reactor design.

1.1.1 Reactor geometry

A Molten Salt Reactor is a controlled environment for a fission chain reaction to occur. A schematic drawing of the reactor is illustrated in figure 2.

In figure 2 three different loops are shown. Relative to a Light Water Reactor (LWR) there is an additional loop. The first loop includes the core, in which the fissile chain reaction is generated. In conventional reactors fissile isotopes, like uranium 235, absorb a neutron. This reaction results into fission products and a large amount of energy, due to a small mass defect which appears as fission energy. In addition, more free neutrons are generated that can be used to continue the chain reaction. A moderator is usually employed to slow down the neutrons, so they are more likely to cause another fission when they impact the fuel. In the case of Light Water Reactors solid fuel rods contain the fissile material. In between those rods a certain amount of control rods are inserted to control the fission chain reaction. Water surrounding the fuel acts as both

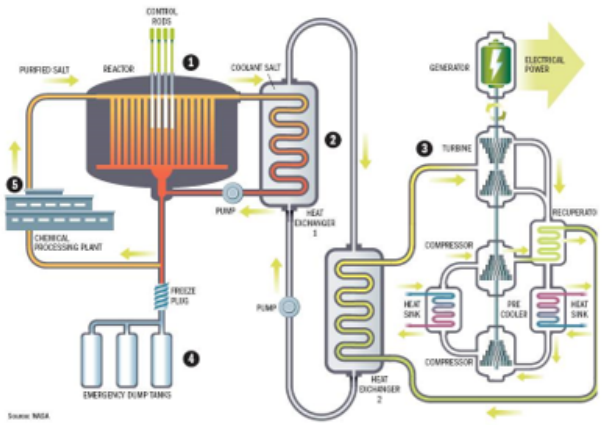

Figure 2: Schematic drawing of the Molten Salt Reactor [10]

a moderator and a coolant. For a MSR a second loop is included. A heat exchanger connects both loops. The coolant in the first loop is heated up and feeded to the heat exchanger. The second loop is also filled with a liquid salt mixture. This loop functions as a heat exchanger and will bring the heat to the third loop via a second heat exchanger. The heat is used in the third loop for heating water to turn a steam turbine to generate electricity. The additional second loop is inserted to separate the steam from the core part of the reactor. In a molten salt reactor the core operates differently. The primary coolant is a salt heated above its melting point, so it is a fluid. Instead of fuel rods fissile material is now dissolved in the molten salt. The fuel salt flows through channels in graphite blocks, which moderate the energy of the neutrons to enhance the chain reactions.

A molten salt reactor can use a broad range of fuel and salt compositions. There are even designs that do not need a moderator at all (fast reactors). Instead of uranium, thorium is a favorite alternative fuel. This is because thorium fuel offers a number of benefits. There is at least three times more thorium than uranium on the planet. Besides that less waste is produced than the waste of uranium. Other benefits include safety and efficiency. Replacing water as the coolant removes the possibility of steam explosions and the generation of flammable hydrogen gas. Additionally, a freeze plug can dump the fuel into tanks and stop the reaction. Because the MSR can operate at higher temperatures their steam cycle generates electricity more efficiently. The use of liquid fuel allows for real time waste processing and finally there is no need to shut down the reactor for refueling. New fuel can be introduced to the system during operation. On the other side, there are also some disadvantages for a MSR. Dissolved fuel can easily come in contact with important equipment, such as pumps, which can be affected. Besides that, there is a risk of corrosion.

1.1.2 Properties, fuel and reactions

For conventional reactors using U-235 the fission reaction is displayed in equation (1.1) [11].

$$ {}^{1}_{0}n + {}^{235}_{92}U -> X + Y + b\,{}^{1}_{0}n \tag{1.1} $$

Here ${}^{1}_{0}n$ is a neutron with mass 1 u. X and Y are the fission products obtained by the fission reaction and b is the number of neutrons released by the reaction. These neutrons propagate the chain reaction. For the MSR the fuel is a point of attention, since it has to meet the important function to be appropriate both as fuel and as coolant. Therefore it will be essential to continuously monitor properties like density and viscosity of the salt for different temperatures. The most commonly proposed fuel salt mixture for the molten salt reactors is $LiF - ThF_4 - UF_4 - PuF_3$. This is a composition of Lithium, Thorium, Uranium and Plutonium fluorides. The melting point of this fluoride salt is around 600 °C, while the MSR operates at a higher temperature of approximately 700 °C and atmospheric pressure. Under these circumstances, especially at high temperature it is hard to know the behaviour of these properties accurately, since standard equipment to measure density and viscosity can not operate well at these high temperatures. There are some practical shortcomings and difficulty of integration in the system for measuring with conventional equipment. Next to that the salts could be corrosive. So a setup using a transducer, which sent a wave throughout a plate into a fluid, can be used. The time between generating and detecting the wave is measured. From this the attenuation of the wave can be calculated, which is a measure for the viscosity of the fluid. This method to measure viscosity uses ultrasonic shear waves. The advantage is that the transducer does not make any contact with the liquid and can therefore operate as usual as it is also less bothered by high temperatures. This will give less trouble. This idea is already tested by Cegla et all [1] and his research is published in 2005.

1.2 Development so far

Up till now a lot of research has been done on measuring properties as viscosity at high temperatures [12]. Besides the research of Cegla et al described above more groups did experiments on ultrasonic waveguide measurements. Below a few are described [1].

First of all, Vogt et al in 2004 published their research on material properties of viscous liquids using ultrasonic guided waves. In this paper they presented a tool in the form of a circular waveguide for measuring the dynamic viscosity as well as the longitudinal bulk velocity (dynamic only takes translational molecular movement into account while bulk reflects on both rotational and vibrational degrees of molecular freedom) . They used a torsional wave in a rod, which is similar to a shear wave in a plate. The set up of this experiment is shown in figure 3. Using different wave modes the material properties can be determined accurately [13].

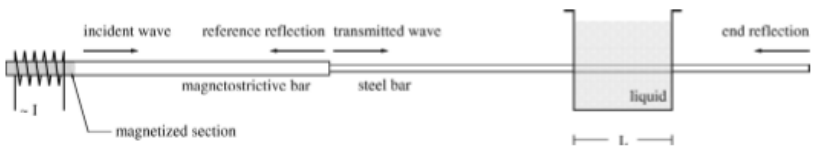

Figure 3: Schematic drawing of the set up used by Vogt et al [13]

Secondly, Rabani et al presented a useful probe for measuring viscosity of Newtonian liquids in 2011. This probe satisfies some issues covered in the research, such as which material the wave guide should have, what the dimensions should be and at what frequency it should operate [14] [15].

Then there is Kazys et al [16] who developed a method using ultrasonic waves to measure viscosity of high viscous substances and non-Newtonian liquids. This research shows which types of wave modes are appropriate and that viscosity is dependent on frequency for high viscous fluids [16].

At last there is the the group of Smith et al, who published their work in 2006. In their research the temperature dependency on the viscosity of five different non-Newtonian fluids were investigated. Also the rheological behaviour of these fluids was investigated. One of the measured fluids is Ethyl Ammonium Nitrate (EAN), which is a powerlaw fluid, is further investigated in this research [4].

1.3 Research and goals

Since the molten salt reactor deals with non-Newtonian salt mixtures it is interesting to have a closer look at the viscous behaviour of non-Newtonian fluids. In this research steps will be taken in investigating these non-Newtonian fluids, EAN, in particular. The set up described by Cegla [1] is used to have a further look at the ultrasonic waveguide method in determination of the viscous behaviour. The main question of this research is:

How does the viscous behaviour and related attenuation by a powerlaw liquid (EAN) act for different high range frequencies of ultrasonic shear waves?

In order to investigate on this question the set up is used. In this set up a thin stainless steel plate functions as a waveguide. At the top of the plate a transducer sends a wave through the plate and is reflected at the bottom. A container with liquid is adjustable to create different immersion depths in which the plate is immersed. By measuring the amplitude of the wave the attenuation of the wave, which is closely linked to the viscous behaviour of the fluid, can be calculated. In supporting the research of finding the answer to the question above some additional subquestions are composed. The first and the last question will both be performed on water and EAN.

1. What is the relation between the viscous behaviour and the immersion depth for both Newtonian and non-Newtonian fluids?
2. Can the theoretical model for powerlaw liquids be simplified to a Newtonian model for certain circumstances?
3. What value for K and n can be found from the theoretical powerlaw model and the literature data from Smith et all [4]?
4. What is the ratio between the signal strength at different frequencies for a fixed immersion depth?

To make sure all these questions can be answered it is necessary to delve into similar literature, test the operation of the setup and analyze measurement results. In the next chapter the theory behind different types of mechanics are explained. Thereafter in chapter 3 the experimental method is presented and the set up is illustrated. In chapter 4 the most important results are stated and discussed. At last, in chapter 5 a conclusion has been drawn and some recommendations for further research are proposed.

Chapter 2: Theory

Before doing measurements on the ultrasonic waveguide it is important to understand the theoretical background behind the experiment. This theory is split up into three parts. The first interest is continuum mechanics, since this explains the kinetics and dynamics of a continuum, which is a body of matter distributed continuously. Besides that wave mechanics is explained. Here the physics behind waves and wavelike properties are discussed. Finally there is fluid mechanics to conclude, which actually is a branch of continuum mechanics and covers mechanics and forces on different types of fluids. Actually these three fields are strongly connected to each other.

2.1 Continuum mechanics

In real life almost every material consists of impurities and discontinuities. However in continuum mechanics, materials are treated as continuous objects. This makes it easier to look at properties of the system at a microscopic level. The experiment deals with vibrations and elastic waves through a fluid and a solid plate. Some essential concepts in understanding these topics and how this propagation works are stress and strain.

2.1.1 Stress and Strain

Stress and strain are two key concepts in speaking about elasticity and both are closely related. Strain basically is the distortion of a homogeneous medium. The origin of strain could be stress, which is an applied force. Stress, to start with, is the measure for a force being exerted on a cross sectional area of the material. However this resulting force is caused by internal collisions and intermolecular forces. This means that particles in the material next to each other apply a force on each other. An example is the various different inter atomic bonds in a molecule, such as covalent bonds or hydrogen bridges.

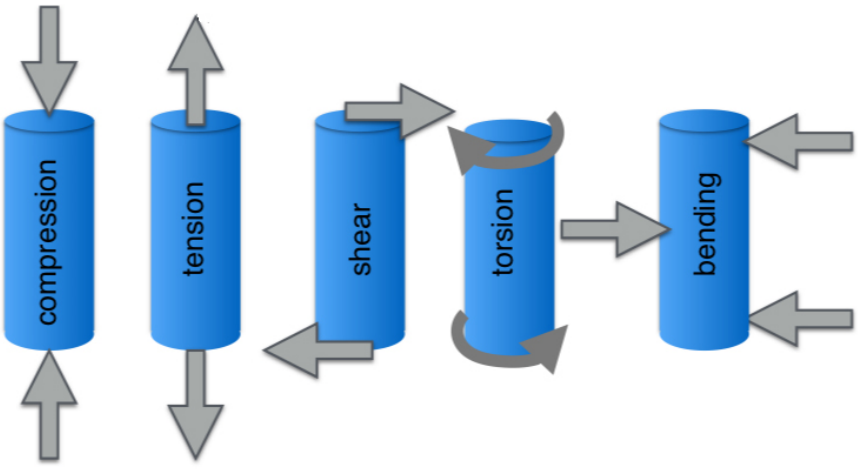

Figure 4: 5 different types of stress, which could be subdivided into normal and shear stress [17].

Stress can be classified into different types, compression, tension, shear, bend and torsion. For compression and tension the applied force is normal to the plane and makes sure a body will stretch or compress. Shear and bend are forces applied on the

body in transverse position. It can cause a material to rotate the surface. Torsion is rotation around the longitudinal axis and can be decomposed into shear forces. So basically stress comes down to two forms, normal stress and shear stress. In figure 4 the five ways of stress are shown.

Stress could be calculated using (2.1).

$$\sigma = \frac{F}{A} \tag{2.1}$$

Hereby F is the force in N, A is the area in m^2 and σ is the stress expressed in N/m^2 [11]. Stress has both a magnitude and direction, this should mean it is a vector. However stress is a tensor. Lets imagine a 2D square solid. Now one force is applied on the left face of the square pointing to the left and another force on the right face pointing to the right. These forces should be equal in order to prevent the body to accelerate infinitely. This will make the square responses in elongating into a rectangle. But if now the forces are applied to the upper and bottom face instead (same magnitude and same direction) the response is different and would look like the figure bottom right in illustration 5.

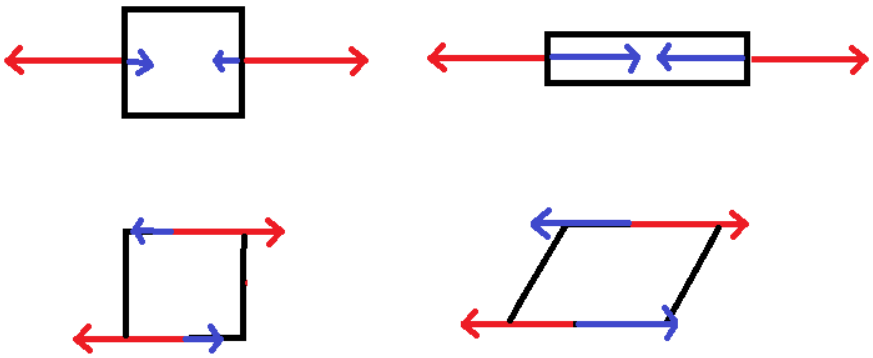

Figure 5: Above: normal forces lead to normal stress. Below: shear forces induce shear stress. The blue arrows are the opposite internal forces. The distortions are called strain.

So this clarifies that not only magnitude and direction matter but also on which face the force acts. This leads to a stress tensor. The stress tensor, which has the symbol T and is called the Cauchy Stress tensor, defines the stress on a body in a certain configuration. A 3D representation of the stress vector components is illustrated in figure 6.

Both the normal stress and the shear stress can be expressed in a matrix (2.2) [19].

$$T_j^{(n)} = \begin{bmatrix} \sigma_x & \tau_{xy} & \tau_{xz} \\ \tau_{yx} & \sigma_y & \tau_{yz} \\ \tau_{zx} & \tau_{yz} & \sigma_z \end{bmatrix} \tag{2.2}$$

The components on the diagonal represent the normal stress and the off-diagonal elements give the shear stress. σ_x gives the stress normal to the y-z plane, while τ_{xz} represents the shear stress parallel to the z-axis in the y-z plane. This will give nine components. Although only six are unique, since the matrix is symmetric. Unequal

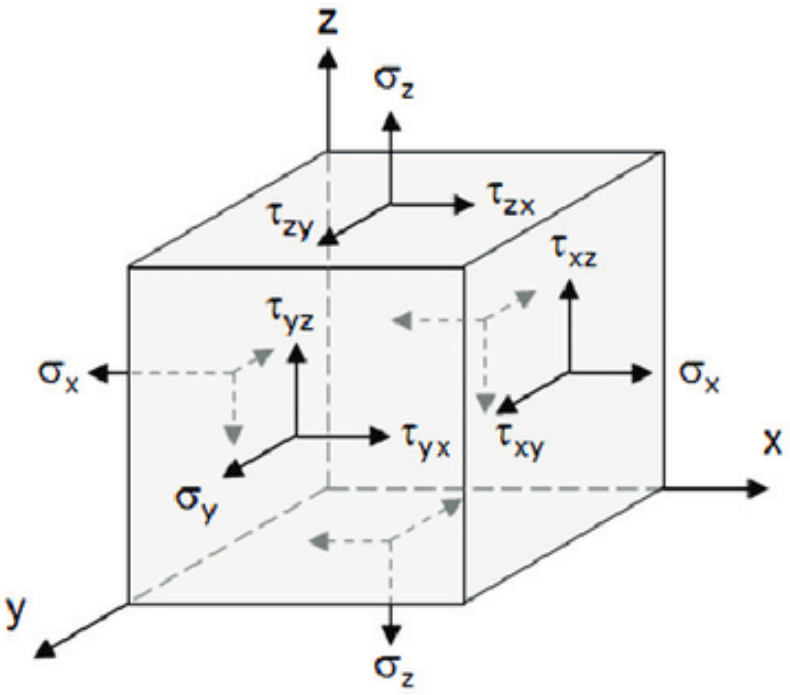

Figure 6: A 3D representation of the stress vector components of the Cauchy Stress Tensor T.[18]

stresses could cause infinite angular acceleration. So instead of a vector with three components this tensor has nine elements. In (2.3) the equation to gain the stress vector on a surface from the stress tensor is displayed.

$$\sigma_{ij} = n_i \cdot T_j^{(n)} \tag{2.3}$$

Here σ is the stress vector and n is the normal vector of the surface. The stress vector is very useful in calculating the total force due to the surface forces over an arbitrary volume (of a fluid for example). Then the stress vector should be integrated over the surface of the volume, see (2.4)[20].

$$F_s = \int_S \sigma_{ij} dS = \int_S n_i \cdot T_j^{(n)} dS \tag{2.4}$$

Here the integral with the stress tensor over the volume is obtained. Furthermore this could be changed into an integral using the divergence of the stress tensor, see (2.5).

$$\int_S n_i \cdot T_j^{(n)} dS = \int_V \nabla \cdot T dV \tag{2.5}$$

The physical meaning of the divergence of a vector field tells in what extent stress flows towards or away from a certain point on the surface of the volume.

As mentioned before, because of these different types of stress a volume can be transformed. This means that particles inside the material have changed their position relative to each other. A measure of the amount of change is strain. Suppose a rod of length l with a constant cross-sectional area A. This rod is stretched until it has a length $l + \Delta l$ by uniformly applied opposing forces. Now the strain of the rod is defined as presented in (2.6) [11].

$$\epsilon = \frac{\Delta l}{l_0} \tag{2.6}$$

Hereby ϵ is the strain, which is dimensionless. l_0 is the original length of the rod in meters and Δl is the change in length relative to the original length also in meters. Similar to stress the strain could also be in the normal direction or parallel to the face of an element. The latter is called shear strain. So as well as for stress a tensor could be defined for strain, which is the Cauchy Strain Tensor. This tensor is written in (2.7) [19].

$$\epsilon_j^{(n)} = \begin{bmatrix} \epsilon_{xx} & \epsilon_{xy} & \epsilon_{xz} \\ \epsilon_{yx} & \epsilon_{yy} & \epsilon_{yz} \\ \epsilon_{zx} & \epsilon_{yz} & \epsilon_{zz} \end{bmatrix} \tag{2.7}$$

Like the stress tensor the strain tensor is symmetric too. Besides that the diagonal elements here also represent normal strain and the off diagonal elements the shear strain. The components in the strain tensor matrix could be calculated using the the formula (2.8).

$$\epsilon_{ij} = \frac{1}{2}(\frac{\mathrm{d}u_i}{\mathrm{d}x} + \frac{\mathrm{d}u_j}{\mathrm{d}y}) \tag{2.8}$$

Here i and j stand for the components x,y and z and u is the displacement vector from the original point to the new point. In gaining this formula the assumption is made that non-linear terms can be neglected, because the gradients of the displacements are very small. The whole derivation of (2.8) is given by [21].

2.1.2 Generalized Hooke's law and moduli

Stress and strain are two closely related concepts, which are described mathematically very similarly. There are some moduli that link stress and strain in a certain environment. First of all the Young's modulus. The Young modulus is a property which gives the rigidity of a solid material. The higher this modulus, the less elastic the material is. Very stiff materials could have a Young modulus of more than a thousand GPa for instance. The modulus describes the response of a material to linear stress. The equation is given in (2.9).

$$E = \frac{\sigma}{\epsilon} \tag{2.9}$$

Here E is the Young modulus in GPa, σ is the stress in N/m^2 and ϵ is the strain, which is dimensionless [22].

For many materials stress and strain could graphically be related to each other in a stress-strain curve. An example is illustrated in figure 7.

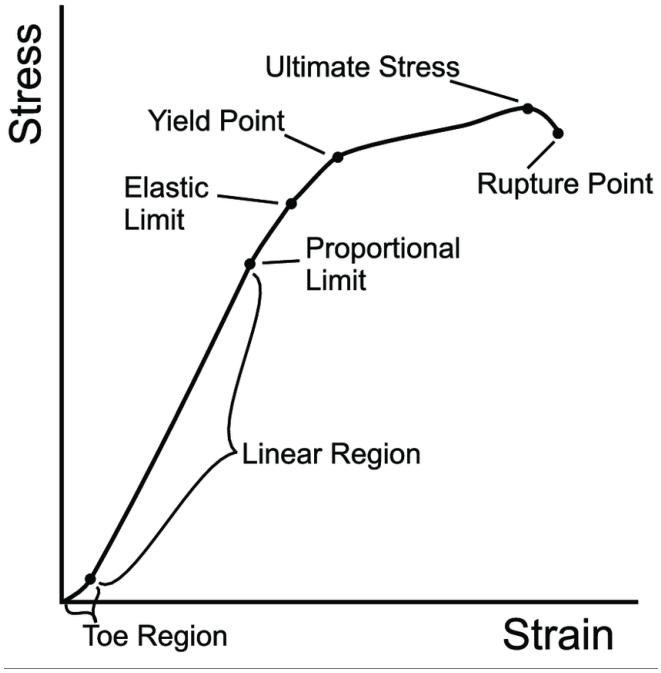

Figure 7: A stress-strain curve where some critical points are indicated. [23]

The linear dependence is shown in the first elastic part of the graph. Then from the elastic limit plastic deformation will occur. The material is now deformed permanently. So it will not return to its original length. This will happen when strain grow faster than stress. Then at a certain point, when increasing the strain the stress will decrease. At this point the material experience maximal tensile strength and then fractions occur.

Secondly there is Poisson's ratio, which is a dimensionless number that compares the transverse strain to the axial strain. This ratio tells how a material responds to contraction and expansion. Most materials expand in one direction if it is contracted in another direction because of preservation of volume of a material. In (2.10) the equation for the ratio is given [22].

$$\nu = -\frac{\epsilon_{trans}}{\epsilon_{axial}} \tag{2.10}$$

Here ν is the ratio and $_{trans}$ and ϵ_{axial} are the transverse and axial strain respectively. Theoretical possible values for the poisson factor lie between $-1 \leq \nu \leq \frac{1}{2}$.

Besides that there is the shear modulus, which relates the shear strain and shear stress. Usually it is expressed in GPa. The equation that describes the shear modulus is given in (2.11) [22].

$$G = \frac{\tau}{\gamma} \tag{2.11}$$

Here G is the shear modulus in GPa, τ is the shear stress and γ the shear strain acting on the material.

At last, there is the Bulk modulus, which is a measure for the compressibility of a material. The equation to calculate the Bulk modulus is given in (2.12) [22].

$$K = -V\frac{\mathrm{d}P}{\mathrm{d}V} \tag{2.12}$$

Here V is the volume of the material or fluid and P is the pressure acting on the volume. Furthermore K is denotes as the Bulk modulus in GPa.

All these concepts describe a certain stress. To predict the deformations of a body all these concepts should be taken into consideration. In the generalized Hooke's law all these contributions are considered [22]. In the following section the focus is shifted towards wave mechanics, which explains different types of waves and propagation through a solid or a fluid. Furthermore additional properties of the fluid could be investigated using the wave equation.

2.2 Wave mechanics

In making a description about waves it is necessary to distinguish electromagnetic waves from mechanical waves. Both types of waves are described as a travelling disturbance and it transfers energy instead of matter, but only electromagnetic waves can travel through vacuum. The velocity of both types of waves differ. Mechanical waves travel less fast, while electromagnetic waves travel with the speed of light in a vacuum. Mechanical waves are used very often in this research.

2.2.1 Types of waves

Mechanical waves come in three different forms, a longitudinal wave, a transverse wave and surface waves.

Longitudinal waves are waves where the amplitude of the wave is parallel to the direction in which the wave propagates the energy. Examples of longitudinal waves are sound waves or pressure waves (P-waves). In both types of waves local compression and extraction causes the propagation of the wave.

Transverse waves are waves where the amplitude of the wave is perpendicular to the propagation of energy of the wave. An example of a transverse wave is light. An important form of transverse waves is shear waves (S-waves). Shear waves could be compared to flexural waves, which are a combination of longitudinal and transverse waves. Both are described in a similar way, only physical properties differ. Flexural waves could be attenuated much more than shear waves for example. This is caused by the fact that shear waves propagates along the narrow side of the plate while flexural waves displace the broad side of the plate. This means that the latter has to displace more surface of the waveguide. Therefore it is attenuated stronger than shear waves.

Surface waves transfer the energy along the interface of different media. It has both characteristics of longitudinal and transverse waves. An example of surface waves are gravity waves. In figure 8 is shown that particles not just moving up and down or

from right to left and the other way around, but move in small elliptical shapes. So the movement of individual particles is a combination of longitudinal and transverse movement [22].

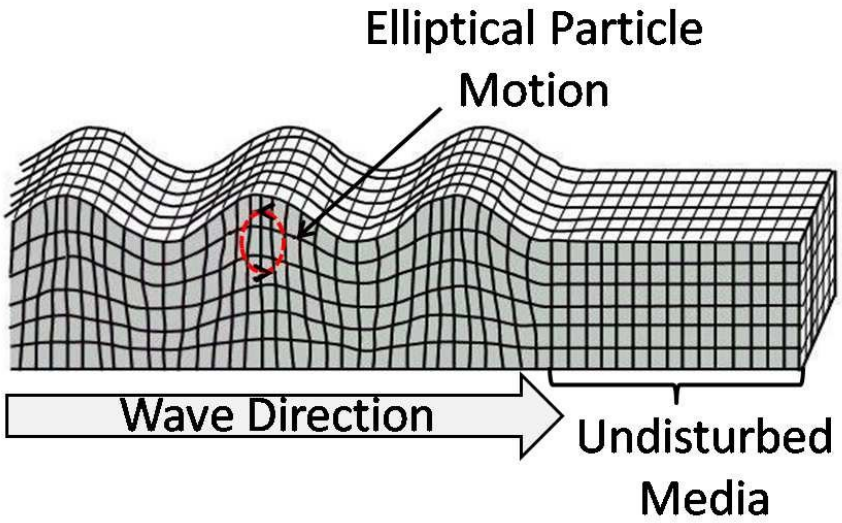

Figure 8: The motion of a mechanical surface wave particle is elliptical. This means it is a combination of longitudinal and transverse movement. [24]

2.2.2 Scholte wave

A special type of waves for this research is the Scholte wave. A Scholte wave is part of the surface wave category and is a particular Stoneley-Scholte wave (which explains solid-solid transitions) [1]. This wave propagates between a solid and a fluid, so a half-space liquid and half-space elastic solid is required. The intensity of the wave decays exponentially when it propagates away from the interface. Besides that, in the liquid the amplitude of the wave does strongly depend on the frequency of the wave. For higher frequencies it is harder for the wave to penetrate into the liquid. This makes sure this type of wave is useful to measure properties of fluids using the high frequency range. However for this research infinite half-space materials do not exist. So to simulate this a plate is immersed into a fluid during this experiment. Under these circumstances a quasi-Scholte wave occurs. This mode approaches the Scholte wave for high frequencies.

2.2.3 The wave equation

Shear waves are very useful to determine the viscosity of a fluid. Viscosity is known as a measure of how much a fluid can resist deformation by shear stress. Shear waves are mechanical waves which induce shear on a material. Shear waves do not propagate within fluids with zero viscosity. The shear wave is attenuated by a few things. Important is the affection by the fluid flowing around the plate. The more viscous the fluid, the more the shear wave is affected. The benefit over other types of waves is that there is no longitudinal leakage. Although shear waves are a bit more difficult to generate and detect. In this experiment a wave generator sends an acoustical

wave through a transducer. This type of wave distributes energy by means of adiabatic compression or decompression. The transducer then excites mechanical waves with horizontal shear polarization through a plate (using the piezo-electric effect). The acoustical wave equation has to be solved in order to gain more information about the viscosity and the attenuation of the fluid. However the wave equation is different for viscous and non-viscous fluids. The 'normal' 3D wave equation of an acoustic wave is given in (2.13) [22].

$$\frac{\partial^2 p}{\partial x^2} - \frac{1}{c^2}\frac{\partial^2 p}{\partial t^2} = 0 \tag{2.13}$$

Hereby p is the pressure field inside the medium, c is the speed of sound in m/s. c is defined in (2.14)

$$c = \sqrt{\frac{K}{\rho_0}} \tag{2.14}$$

where K is the bulk modulus in GPa and ρ_0 is the density in kg/m^3. For viscous fluids the wave equation is given in (2.15).

$$\nabla^2 p - \frac{1}{c^2}(\frac{\partial^2 p}{\partial t^2} + \frac{4\mu}{3\rho}\frac{\partial \nabla^2 p}{\partial t}) \tag{2.15}$$

An additional term, including the viscosity μ of the fluid, is obtained by the evaluated Navier-Stokes equation. For both equations a solution for p could be derived by solving the partial differential equations. First of all, equation (2.13) is solved using separation of variables, which results in a sinusoidal plane wave function (2.16).

$$p(x,t) = p_0 e^{\pm i(kx-\omega t)} \tag{2.16}$$

Here p_0 is the pressure at the initial conditions, ω is the angular frequency and k is the wavenumber, which is defined as $\omega = kc$. The derivation of the other partial differential equation is more difficult but it will give a similar solution for p, only the dependence on both ω and k change. The formula for k for example is turned into the complex equation of the form (2.17), where α is the attenuation.

$$k = \pm(\beta + i\alpha) \tag{2.17}$$

This α has the unit of m^{-1} and does depend on the viscosity of the fluid. For this research the attenuation is given by (2.18).

$$\alpha = -\frac{1}{2h}(\frac{2\rho_f \omega \eta}{\rho_s G})^{\frac{1}{2}} \tag{2.18}$$

Here h is the immersion depth of the plate, ρ_f is the density of the fluid in kg/m^3, ρ_s is the density of the plate in kg/m^3 and G is the shear modulus of the plate in GPa [25]. Another more intuitive detailed derivation of the attenuation α of (2.18) using a balance over the plate is given in Appendix A.

2.2.4 Attenuation and viscosity determination

By looking back at equation (2.18) the only parameter that is unknown in order to calculate the viscosity μ is the attenuation α. To find the attenuation a more in depth analysis of the path of the wave is necessary. In fact the attenuation of the wave is the relative decrease in amplitude. In figure 9 a schematic representation of a plate immersed into a fluid is displayed.

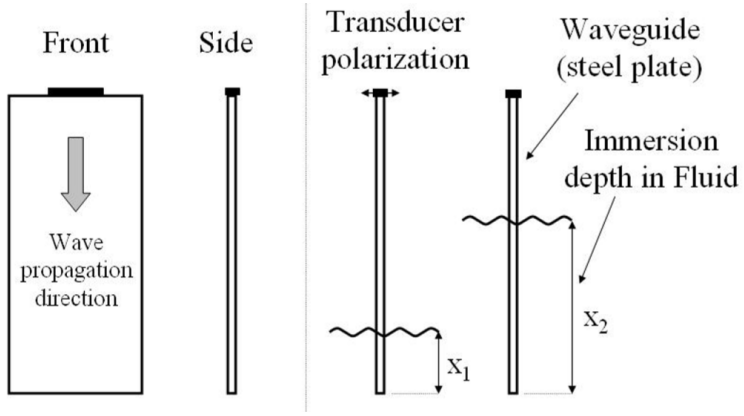

Figure 9: Schematic representation of the plate immersed into the fluid using a waveguide plate.[1]

The transducer propagates a wave downwards into the plate, it is reflected at the bottom and measured back at the transducer. Along this path the wave is attenuated in three different ways. Firstly by the plate itself, which affects the amplitude of the wave exponentially. Secondly the transition at the interface between the solid of the plate and the fluid. A certain part of the wave is transmitted, while another part is reflected. At last the attenuation caused by the fluid, which for water for instance has also an exponential decaying dependence[1]. In (2.19) the three influences are expressed into an equation.

$$A_1 = A_0 e^{-\alpha_{plate} 2 l_{plate}} T^2 e^{-\alpha_f 2 l_1} \tag{2.19}$$

Here l_{plate} is the length of the solid, l_1 is the length the wave travels inside the fluid, α_{plate} is the attenuation of the solid, T is the transmission coefficient and α_f is the attenuation of the fluid, which is the subject of interest. The lengths are doubled because the wave travels back and forth trough the plate. For the same reason the transmission coefficient is squared. The wave crosses the solid-fluid interface twice. In (2.19) there are lot of parameters which are already measured, such as both l values as well as both amplitudes. However α_f is not the only unknown, so solving for this parameter is difficult. This problem could be solved by setting up (2.20) for another immersion depth.

$$A_2 = A_0 e^{-\alpha_{plate} 2 l_{plate}} T^2 e^{-\alpha_f 2 l_2} \tag{2.20}$$

The term including the exponent of the plate is very small compared to the other terms since the attenuation of the plate is very small. If both equations are now equated these parameters will cancel out, written in (2.21).

$$\frac{A_1}{e^{-\alpha_f 2l_1}} = \frac{A_2}{e^{-\alpha_f 2l_2}} \tag{2.21}$$

Now the α_f is rewritten and evaluated by (2.22).

$$\alpha_f = \frac{1}{2(l_2 - l_1)} ln(\frac{A_1}{A_2}) \tag{2.22}$$

So this means one should only measure the lengths and amplitudes at two different immersion depths to calculate the attenuation of the fluid and with that the viscosity of the fluid can be calculated using (2.18) [25].

2.3 Fluid mechanics

The last part of the theoretical section is covered by fluid mechanics, which explains the physical behaviour of fluids if forces act on them. As already mentioned before, physics becomes different in working with viscid or inviscid flows. The derivation in Appendix A for example only holds for a special type of fluids. For this research therefore it is necessary to distinguish two types of fluid: Newtonian and non-Newtonian fluids.

2.3.1 Newtonian model

Newtonian fluids are liquids where shear stress and viscosity are related linearly. Furthermore the viscosity of Newtonian fluids does not change with the amount of shear under constant temperature conditions. The most common examples of a Newtonian fluids are air and water. Those fluids adhere to Newton's law of viscosity, as could be seen in (2.23).

$$\phi''_{p_y,x} = -\mu \frac{\mathrm{d}v_y}{\mathrm{d}x} \tag{2.23}$$

Here $\phi''_{p_y,x}$ is the flux of y-momentum, v_y is the velocity of the y component and μ is the viscosity of the fluid [26].

2.3.2 Powerlaw model

Then there are non-Newtonian fluids, which are more common than exception. They do not obey Newton's law of viscosity. There are a lot of different types of non-Newtonian fluids with all their own so-called rheology, meaning the dependence of the shear stress and the velocity gradient. One common type is the powerlaw liquid. Examples of powerlaw liquids are cement or styling gel. They both obey the powerlaw, given in (2.24).

$$\tau_{xy} = -K \mid \frac{\mathrm{d}v_y}{\mathrm{d}x} \mid^{n-1} \frac{\mathrm{d}v_y}{\mathrm{d}x} = -K \mid \frac{\mathrm{d}v_y}{\mathrm{d}x} \mid^{n-1} \dot{\gamma} \tag{2.24}$$

Hereby τ_{xy} is the shear stress, K is the consistency in Pas^n, $\dot{\gamma}$ is the shear rate and n is the flow index. n is dimensionless. For n equals 1 the fluid is Newtonian. This is

a special case. When n is smaller than 1 the liquid is called shear-thinning. For n is bigger than 1 the fluid is called shear-thickening. For the latter the apparent viscosity, which is defined in (2.25), increases at higher values of the shear rate.

$$\mu_{app} = K \mid \frac{\mathrm{d}v_y}{\mathrm{d}x} \mid^{n-1} \tag{2.25}$$

In figure 10 the shear rate is related to the shear stress for different values of n. In this experiment water as well as a powerlaw liquid is used and compared [26].

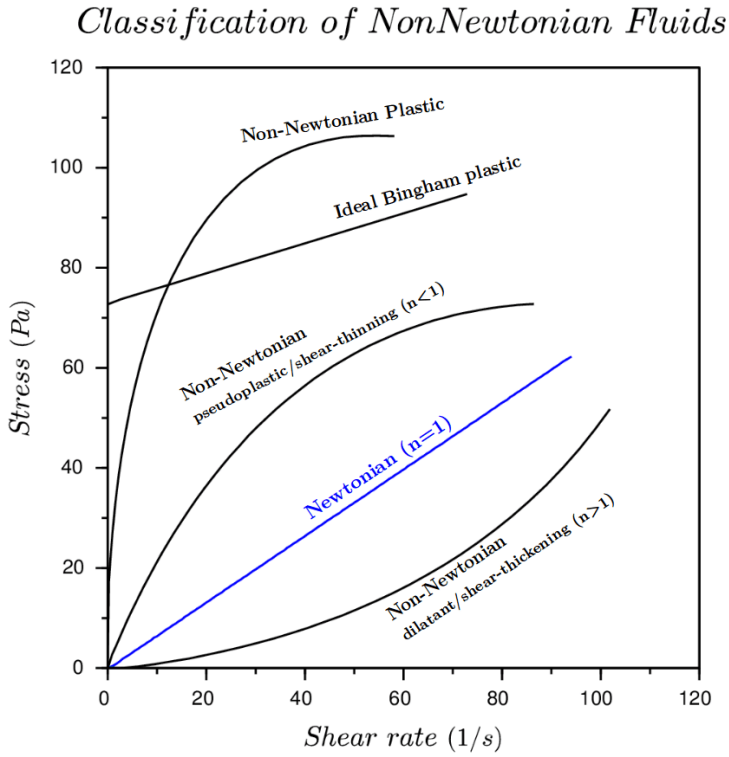

Figure 10: The shear stress for different values of shear rate. The blue line represents the Newtonian model (n=1). [27]

In the following section the experimental setup and the used methods are described in detail.

Chapter 3: Experimental method

To achieve the research goals and answer the research question a set up is used. The experiment follows the procedure of Cegla et all [2].This method is based on ultrasonic waveguide. A schematic illustration of the whole set up is displayed in figure 11.

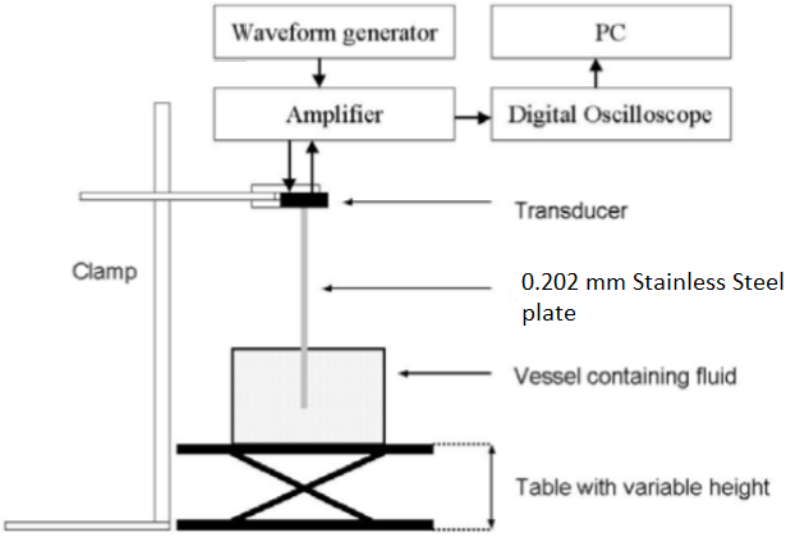

Figure 11: Schematic representation of the used setup [1]

A signal generator is used to generate a shear wave in the range from $2 - 5MHz$. After amplification it is sent to the transducer. It is an horizontal shear wave. The transducer sends the wave into the wave guide and detects it after reflection. The detected signal then goes to the oscilloscope, where the wave is displayed, as well as the original generated wave. In between the wave passes a delimiter, which makes sure the voltage entering the oscilloscope is maximal $1.0V$. A photo of the used setup is given in figure 12.

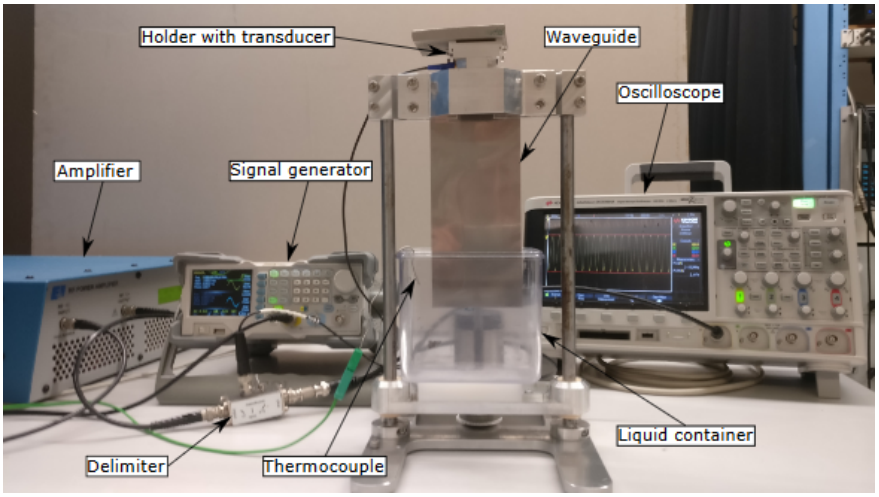

Figure 12: The used setup to determine the viscosity of a fluid. [2]

3.1 Setup design

The wave pulse created by the waveform generator is a sinus. The pulse consists of 40 periods with a certain frequency, which is varied between $3.0MHz$ and $5.0MHz$ for this experiment. After $30ms$ another pulse is generated. This time is necessary to avoid interference between the wave pulses. Each wave pulse is deflected at the end of the plate and returned towards the transducer to be detected. The used generator is a RIGOL DG1032Z. After the signal is generated it passes an amplifier. This is because the oscilloscope and the transducer deal with much greater input voltages. The maximum input voltage of the oscilloscope is 200 V_{pp}. The signal generator can output pulses with a voltage of an order of magnitude smaller. So therefore the signal is amplified. However the amplifier is limited by an input signal of $2\sqrt{2}V_{pp}$. For safety reasons an input signal of $1V_{pp}$ is chosen. This voltage is amplified approximately 300 times. However this amplification will damage both the oscilloscope and the transducer. For this reason the amplitude of the signal is decreased by a delimiter.

From the delimiter the wave is sent towards the transducer, which is coupled at a plate. The transducer converts the acoustical or electrical wave into a mechanical shear wave. This is done using the reversed piezoelectric effect. This means an outer electric field either stretches or compresses the material. The mechanical shear wave then propagates through a wave guide. The wave guide is a plate of stainless steel. The dimensions of the plate are given in table 1 in the results section. The width of the plate is measured using a caliper with accuracy $0.02mm$. The length is measured by a ruler with accuracy $0.1mm$ and the thickness by a caliper with accuracy $0.002mm$. The mass of the plate is measured by a scale with an accuracy of $0.01gram$. The size of the plate should be optimized. It should be as long as possible to fit inside the setup, since the more the plate could be immersed into the liquid the more measurements could be done. Besides, the width should be at least larger than the width of the transducer and the thickness should be small, because small plates attenuate more than thicker plates. The plate is rigidly connected with the transducer in order to attenuate the wave as little as possible. The couplant also should transmit shear waves. Therefore it may have a high viscosity. The transducer should be connected perpendicularly to the plate. The used transducer has a peak frequency of $3.7MHz$. This means the Signal to Noise Ratio (SNR) is the best for this frequency [21].

Another important issue is the attenuation of the wave by other stresses. It is good to know that the wave, which propagates through the plate is quite centered along the plate. This means affecting the plate in this region will attenuate the wave enormously, while affecting the sides of the plate will hardly have any effect at all.

When the wave is reflected and detected by the transducer the mechanical attenuated wave is converted back in a electrical or acoustical wave. The mechanical wave makes sure positive and negative charges shift and cause an external electric field. This electrical wave travels towards the oscilloscope. This is a Keysight InfiniiVision DSOX2024A oscilloscope. The oscilloscope displays both the original generated signal as well as the attenuated reflected wave signal. How the data is analyzed is discussed in section 3.2.

3.1.1 Properties of the liquids and the container

For this research the plate is immersed into a container filled with a fluid. Two different containers and fluids are used. The dimensions of the containers are given in table 2 in the results section.

The length, width and height of the containers are measured by a caliper with an uncertainty of $0.02mm$. The first container has a much bigger volume compared to the other container. Inside the container a thermocouple is placed to measure the temperature during the experiment. Viscosity does strongly depend on temperature. The thermocouple is calibrated using ice water and boiling water.

The large container is used for the experiment with water. Water is a Newtonian fluid. The attenuation derived in (2.18) in appendix A is also based on experiments with a Newtonian fluid. Using this alpha an accurate exponential fit could be plotted along the measurements. From this exponential fit the viscosity can be obtained. For non-Newtonian fluids the derivation will result in an apparent viscosity. The actual viscosity does depend on the shear rate. In this experiment the powerlaw fluid Ethyl Ammonium Nitrate (EAN) is used. EAN is a shear thinning liquid. Because the actual MSR deals with non-Newtonian salts EAN is used as a model fluid. A lot of properties of EAN should still be investigated, such as the rheology of the fluid. EAN, which has the formula $C_2H_8N_2O_3$, is colorless, has a molar mass of $108.1g/mol$ and a density of $1.261g/mL$. Besides that, the fluid has some hazards [28], therefore goggles and gloves are used during the measurements. Because EAN is a bit hazardous and expensive the smaller container is used for these measurements.

3.2 Data analysis

Once the data is displayed at the oscilloscope the part of interest is the first reflection of the wave. The data of this part could be converted into comma-separated values (csv) files, where the measured voltages as well as some key parameters such as temperature are saved. This is done by a LABVIEW script. In this script the amount of snapshots or wavepulses is set as well as the time between these pulses or snapshots.

3.2.1 Labview program

For this research the common amount of measured snapshots is 256, where each consists of a certain number of full periods. The number of periods does depend on the frequency of the wave. The signal is measured for the following frequencies: $3.0, 3.5, 4.0, 4.5$ and $5.0MHz$.

In order to reduce noise in the signal of the amplitude of the measured snapshots, the pulses are averaged after detection. This is done by taking the mean of all 256 pulses to create a signal with a relatively stable amplitude and less noise. The background noise is assumed to have a fixed variance and zero mean, so this will cancel out. Afterwards the root-mean-square value of the wave is calculated to find a measure of the amplitude of the wave. For a sine wave the RMS value is given by the amplitude divided by $\sqrt{2}$ (the noise is neglected). This last factor will cancel out in (2.22) due to the division inside the logarithm. Therefore using the RMS value is a effective method during this experiment. The actual definition of the RMS is given in (3.1) [29].

$$S_{rms} = \sqrt{\frac{\sum_{m=1}^{M} S_i^2}{M}} \tag{3.1}$$

Here S is the signal strength in volts and M is the total amount of measured data points. m is given as the index of a certain data point.

Not all measured snapshots are good representations and some are not useful to contribute to this average. These measured snapshots have to be taken out. Some criteria are introduced to gain the most accurate results:

1. If the RMS value of the wave pulse is smaller than the RMS value of all snapshots added up together, then the snapshot will be removed because the pulse is not assigned as a complete reflected wave packet.
2. If the phase is completely reverted compared to the (average of the) other snapshots it will be removed as well. Otherwise it will cancel out against the other 'good' snapshots. This will be checked by comparing the RMS value of a certain part of the wave with the total averaged wave. If this difference is bigger than a threshold number the snapshot is removed. Especially if the wave pulse starts at a peak this is a valuable control, because the phase is harder to find at this point due to noise around the peak.

The filtered incorrect snapshots are removed from the data and the other correct snapshots are used to calculate the viscosity of the fluid.

3.2.2 Calibration

The LABVIEW script also regulates the immersion depth of the plate via a motor. The motor makes sure the container lifts and goes down. Calibration is needed, since for the big container the level of the fluid does not change significantly by immersing the plate, while for the small container this effect has a major contribution. For the calibration the assumption is made that the liquid level of EAN scales linearly with the depth of the immersed plate.

The maximal change in immersion depth during the experiment is $50.0mm$. For this rise the motor takes 96000 steps. In the program the amount of motor turns is a common measure to change the height of the plate. Each turn corresponds to 1600 steps (so the total rise is 60 motor turns). For the big container each motor turn will make the plate rise $0.833mm$. Therefore the depth of the plate increases $5.0mm$ per 6 motor turns. For the smaller container the level of the liquid rises a bit if the plate is immersed due to less volume in the container. This gives an extra rise of $0.6mm$ for 49 motor turns. For each mm the plate is immersed, it will be immersed an extra $0.0142mm$ because of this volumetric rise. This means that per motor turn the extra rise of the liquid is $0.01224mm$. For 50 motor turns the liquid level then is increased by $0.71mm$. So for the the small container each motor turn will make the plate rise $0.833+0.01224 = 0.845mm$.

3.2.3 Viscosity determination

During the experiment 13 measurements are done at different immersion depths. These points are equally spaced. A MATLAB program is used to gain the viscosity and

attenuation of a Newtonian fluid using (2.18). For a Newtonian fluid the amplitude attenuates exponentially. The RMS amplitude at these 13 points are measured. Using these values the exponential function of (3.2) is fitted against the data points (the derivation for this exponential is given in appendix A).

$$S(z) = ae^{-b(z-z_0)} \tag{3.2}$$

In this formula a and b are the fit parameters. Those values will be optimized using the measured data points. The constant a is the magnitude of the amplitude for a clear dry plate. The constant b is the attenuation ($\alpha_f = \frac{b}{2}$) and is affected by the shear modulus and the density for instance, see (2.18). The viscosity is calculated using this parameter.

A value for the attenuation and the viscosity can also be determined using only two different measured depths. Then (2.22) is used to calculate the value for α. However this method is less accurate, since it is based on only two datapoints. Systematic errors are then a lot harder to notice.

For powerlaw liquids the exponential from equation (3.2) is not valid anymore, since the derivation from appendix A is based on Newtonian fluids. In order to determine the attenuation of a powerlaw liquid (2.22) is used. Between each two measurements the attenuation can be calculated using the signal strengths at these depths. With this attenuation an apparent viscosity can be obtained. In section 4 a model by Rohde [20] is given to calculate the attenuation of a powerlaw liquid with the corresponding amplitude of the signal. This model depends on two parameters n and K, which are the flow index and the consistency, respectively.

3.2.4 Uncertainty

The determined values for the viscosity will bring a certain uncertainty. The explicit formula to calculate the viscosity is given in (3.3).

$$\eta = \frac{2\alpha^2 \rho_s G h^2}{\rho_f \omega} \tag{3.3}$$

All the parameters included have an uncertainty. This makes sure the error is propagated as displayed in (3.4) [29].

$$\frac{\epsilon(\eta)}{\eta} = \sqrt{(\frac{2\epsilon(\alpha)}{\alpha})^2 + (\frac{2\epsilon(h)}{h})^2 + (\frac{\epsilon(\rho_s)}{\rho_s})^2 + (\frac{\epsilon(G)}{G})^2 + (\frac{\epsilon(\rho_f)}{\rho_f})^2 + (\frac{\epsilon(\omega)}{\omega})^2} \tag{3.4}$$

In this formula the error of the thickness of the plate is caused by the caliper, which has an uncertainty of $0.002mm$. The deviation of ω is given by the oscilloscope and is $0.1Hz$. The error is then calculated by dividing the deviation of omega by omega. The error in the density of the solid and the fluid are given in (3.5) and (3.6).

$$\frac{\epsilon(\rho_s)}{\rho_s} = \sqrt{(\frac{\epsilon(l)}{l})^2 + (\frac{\epsilon(h)}{h})^2 + (\frac{\epsilon(w)}{w})^2 + (\frac{\epsilon(m_s)}{m_s})^2} \tag{3.5}$$

$$\frac{\epsilon(\rho_f)}{\rho_f} = \sqrt{(\frac{\epsilon(V)}{V})^2 + (\frac{\epsilon(m_f)}{m_f})^2} \tag{3.6}$$

Here the width has an uncertainty of $0.02mm$ and the height has an uncertainty of $0.1mm$. In addition the uncertainty of the volume of the fluid is $0.04mL$ and the uncertainty of both masses (the fluid and the plate) is $0.01g$.

For the error in the shear modulus it is good to know that besides (2.11) the shear modulus also has another definition which depends on the density ans the velocity. This definition is given in (3.7).

$$G = v_s^2 \rho_s \tag{3.7}$$

The velocity v_s is defined as the path length divided by the travel time. The travel path is defined as two times the length of the plate, while the time is measured by the oscilloscope with uncertainty of 0.1 ms. This is the reading error at the scope. So the error of the shear modulus is calculated by formula (3.8), using (3.9) and the fact that the deviation in t is $0.1s$.

$$\frac{\epsilon(G)}{G} = \sqrt{(4\frac{\epsilon(v_s)}{v_s})^2 + (\frac{\epsilon(\rho_s)}{\rho_s})^2} \tag{3.8}$$

$$\frac{\epsilon(v_s)}{v_s} = \sqrt{(\frac{\epsilon(l)}{l})^2 + (\frac{\epsilon(t)}{t})^2} \tag{3.9}$$

At last, the error in alpha is needed to gain the error in μ. This uncertainty is gained from the MATLAB script. The error of the attenuation is obtained from 95% confidence bounds of the obtained fit value for the attenuation [29].

In the next section the obtained results are illustrated and discussed.

Chapter 4: Results and Discussion

In the previous sections the experimental setup and research goals are described. Below the findings are presented, starting with the measurements of water based on the Newtonian model. All results are processed by MATLAB. The dimensions of the used parameters for both the plate and the containers are taken from table 1 and 2.

Table 1: The dimensions of the stailess steel plate.

Property	Dimension
length $l[mm]$	203.5
width $w[mm]$	80.2
thickness $d[mm]$	0.202
mass $m[g]$	25.96
density $\rho_s[kg/m^3]$	7876
Shear modulus $G[GPa]$	74.86

Table 2: The dimensions of the used containers.

Property	Big container(Water)	Small container(EAN)
length $l[mm]$	119.8	110.6
width $w[mm]$	65.1	6.3
height $h[mm]$	109.0	81.4
maximal volume $V[mL]$	850.1	56.7

Besides that, for EAN the density of 1261 kg/m^3 is used and for water the formula (4.1) below is used to calculate the density [30].

$$\rho_f = \frac{A}{B^{1+(1-\frac{T}{C})^D}} \tag{4.1}$$

Here the values of A,B,C and D are 99.3974; 0.310729; 513.18 and 0.305143 respectively. T is the temperature in K. The temperature is measured constantly during the experiment by the thermo couple.

4.1 Newtonian fluids

Each measured csv file consists of the important measured parameters, such as temperature and density, as well as 256 snapshots of the wave. All those voltages are saved in this file. In figure 13 only one snapshot is shown.

This snapshot has a pre-entered frequency of 4.0 MHz. The amplitude is quite stable, however there is still some noise. This could be seen at the peaks of the sine wave. For this frequency the pulse, which is a complete wave packet, consists of approximately 20 periods. For higher frequencies this should be more and for lower frequencies it should be less.

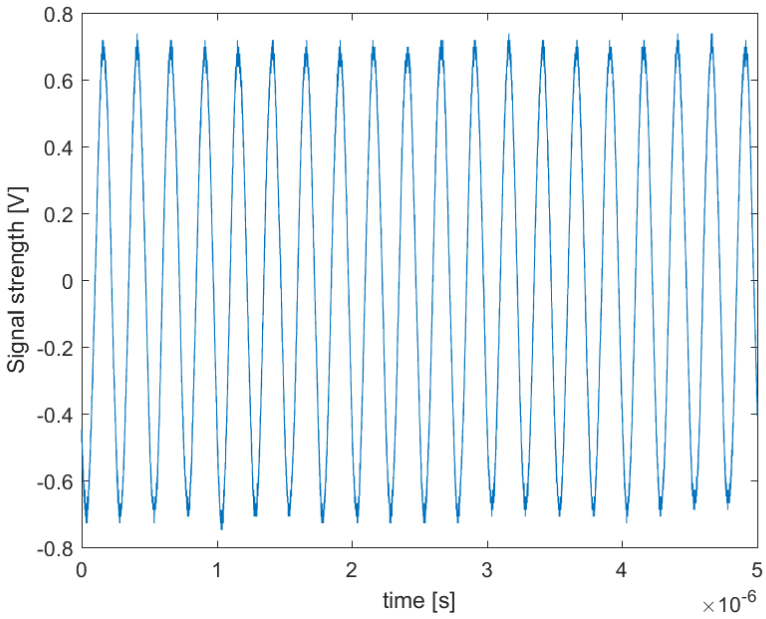

Figure 13: A single snapshot measured at a frequency of 4.0 MHz

4.1.1 Attenuation and Viscosity

In order to visualize the attenuation of the RMS value of these measured snapshots it is necessary to calculate the RMS values for different immersion depths. Then an exponential is fitted and optimized in order to match the data best. For a measurement using a wave of 4.0 MHz and the big container filled with water the data points and exponential fit are shown below in figure 14.

From figure 14 it becomes clear that the exponential fit looks very linear. This is caused by the fact that only the very first small part of the exponential is displayed. So if one needs a wider range it is necessary to extend the plate for example. This makes sure a more immersion depths could be investigated, resulting in more accurate and spreading outcomes. Another option to gain a wider range of measurements is to use a more viscous fluid instead of water. Because the exponential decays faster it becomes clear the data points are more spread along the curve.

By looking at more curves at different frequencies it is remarkable that the first data point often deviates from the other data points (like in figure 14). This could be caused by the fact that the level of the plate is not calibrated very well. The plate, for instance, hangs a very small distance above the liquid interface. This makes sure the first immersion depth becomes a bit smaller (since the plate first has to cover a very small distance through the air until it is submerged in the liquid) then the expected value for z. This would result in a little smaller calculated viscosity. So it causes a small systematic error and therefore these points are taken out in this research. The uncertainties of the data points are given in figure 14. These are calculated by equation (4.2) [29].

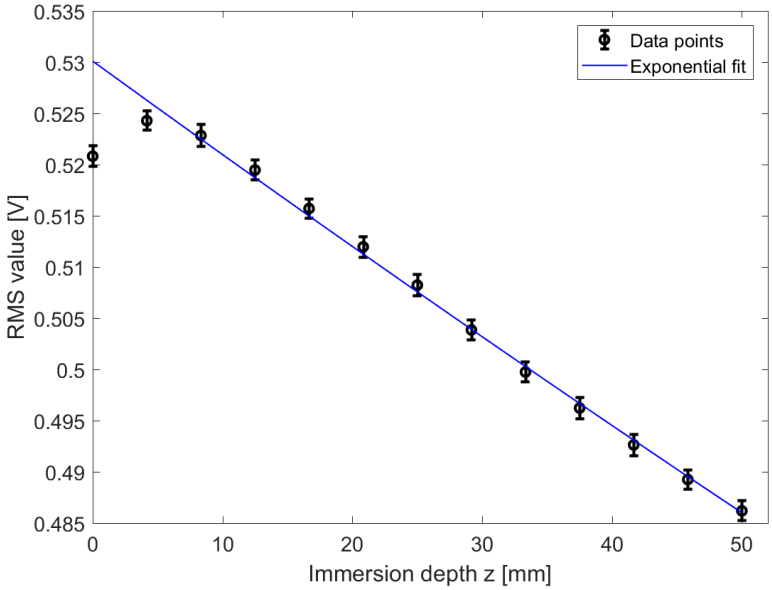

Figure 14: The RMS values in V for different immersion depths in mm with standard deviation. The blue line is the fitted exponential with parameters $a = 3.012 \pm 0.227\ V$ and $b = -1.737 \pm 0.073\ m^{-1}$. For the fit the first data point is not taken into account.

$$\sigma_{N-1} = \sqrt{\frac{1}{N-1}\sum_{i=1}^{N}(x_i - \bar{x})^2} \tag{4.2}$$

Here N is the amount of snapshots, i is the index of a given snapshot, x_i is the RMS value of the i-th snapshot and $\bar{x}$ is the mean of the RMS values of all snapshots. The order of magnitude of the error is approximately $0.001V$. The uncertainty in the fit parameters are calculated by MATLAB. The errors for a and b, as defined in equation (3.2) (using $z_0 = 0$), are 0.227 and 0.073 respectively. From figure 14 it becomes clear that the amplitude decreases if the immersion depth increases. This is not surprising since the wave experiences more resistance from the water surrounding the plate. The value of α is given by the b value of the fit, in this case $\alpha = -1.737 \pm 0.227\ m^{-1}$. Given this value the viscosity, calculated, using (3.3), becomes $\eta = 1.4419 \pm 0.0883\ mPa\ s$. Actually only two data points and signal strengths are necessary to calculate the attenuation (see equation (2.22)) , but using more data clearly gives a more accurate result. If someone determines the attenuation and viscosity between all subsequent data points the result will give a lot of fluctuations between the determined values for the viscosity. This is because a small change in signal strength, caused by noise or a disturbance in the setup, will results in big changes in the measured viscosity. All measurements for water at different frequencies including the calculated attenuation and viscosity, using the fit and the calculation based on (2.18) and (2.22) (where the first and last measurement are used to get the biggest change in immersion depth), are given in table 4 and 5 in Appendix B (here the first data point is taken into account).

If all measured values for the viscosity are averaged for the different frequencies a graph could be made, which is illustrated in figure 15.

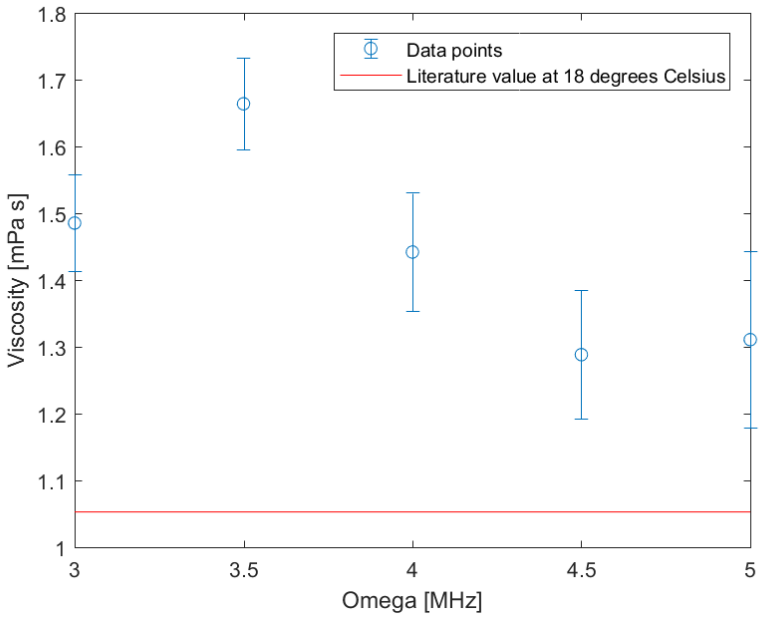

Figure 15: The viscosity at different frequencies. The error bars are included. The red line represents the literature value of the viscosity of water at 18 ° C. This is 1.0526 $mPas$.[31]

In the figure the uncertainties are displayed as well as a red line representing the literature from IAPWS 2008[31]. This line is based on a temperature of 18 ° C. This is a flat line, since the viscosity of water should not change for different frequencies. However the viscosity does depend on temperature. This is illustrated in figure 16.

In figure 16 the temperature is set on the x-axis and the viscosity on the y-axis. The red line has a small slope now. The literature data is based on IAPWS 2008[31]. Here is stated that the viscosity will be less for high temperature. However the opposite is shown in figure 16. For the experiments both the blue and purple data points increase at higher temperatures. A possible reason is the fact that the plate was not dry before the start of a measurement. This causes the viscosity to be higher than expected. The uncertainty of the values of the viscosity is calculated by (3.4). One should expect the lowest uncertainty near the peak frequency, which is 3.7 MHz, since the power loss of the signal from the transducer is here the lowest[21]. However this is not visible in figure 15. An uncleaned wet plate could as well be a possible reason to cause this effect. The fact that during the first measurements the plate was not cleaned after each experiment affects the measurements a lot. It means that the plate is covered with residual fluid. This has a large effect on the following experiment as well on powerlaw fluids, since only this small layer of fluid still can attenuate the wave. By doing the experiments on EAN the plate is cleaned after each measurement. So the effect should be less.

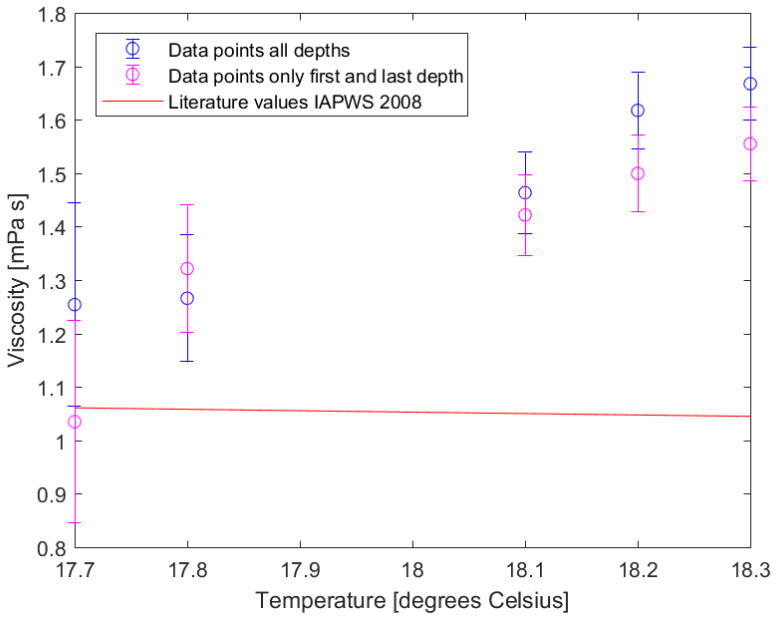

Figure 16: The viscosity at different temperatures for several frequencies. The error bars are included. The blue points are calculated using all depths with (2.18) and the purple points using the first and last depth (formula (2.22)) The red line represents the literature value of the viscosity of water.[31]

4.2 Powerlaw fluids

In the MSR a molten salt is used, which is a non-Newtonian fluid. The behaviour of the viscosity of EAN, which is a powerlaw fluid, is investigated in this research. The rheology of a powerlaw fluid is given in (4.3) [26].

$$\tau_{xy} = -K \mid \frac{\mathrm{d}v_y}{\mathrm{d}x} \mid^{n-1} \frac{\mathrm{d}v_y}{\mathrm{d}x} = -\mu_e \dot{\gamma} \tag{4.3}$$

Here $\mu_e = K \mid \frac{\mathrm{d}v_y}{\mathrm{d}x} \mid^{n-1}$ and $\dot{\gamma} = \frac{\mathrm{d}v_y}{\mathrm{d}x}$. Compared to a Newtonian fluid another parameter K, the consistency, has appeared. Besides that, often an effective or apparent viscosity is defined as in (4.3). This is not constant and depends on the shear rate $\dot{\gamma}$, which is defined in (4.3). For this experiment the shear rate at the solid-liquid interface is given in (4.4)

$$\dot{\gamma_{0,N}} = \frac{B(z)\sqrt{2}}{\delta} cos(kz - \omega t - \frac{\pi}{4}) \tag{4.4}$$

where $\delta = (2\eta/\rho_f\omega)^{1/2}$ is the so-called viscous skin depth. The order of magnitude is a few micrometers.

As powerlaw liquid EAN was chosen because it was immediately available. Besides that it has some properties in common with water, forming hydrogen bonding networks and micelles for instance. In addition a few literature data was available regarding rheology and it has some preferred properties, such as being liquid at room temperature.

However there are some disadvantages. EAN is hazardous and has safety consequences, like skin and eye irritation. Another drawback is that the actual rheology of EAN is unknown. Although the behaviour is tested and for a frequency of 4.0 MHz the graph of the signal strength at different immersion depths is shown in figure 17. The uncertainty of the data points are calculated using (4.2). All measurements for EAN at different frequencies including the calculated attenuation and viscosity, using the Newtonian fit (3.2) and the calculation based on (2.18) and (2.22) (where the first and last measurement are used to get the biggest change in immersion depth), are given in table 6 and 7 in Appendix B.

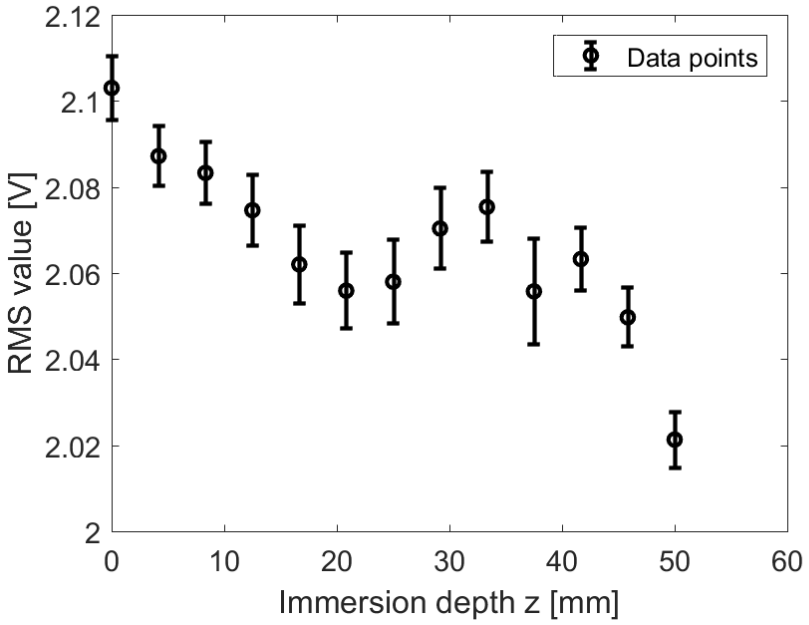

Figure 17: The RMS values of EAN in V for different immersion depths in mm with standard deviation.

By looking at the figure some remarkable things come up. First of all the trend of the data points. The signal obviously attenuates faster than the measurement of water at the same frequency in figure 14. At the same time it is usual for all other measured frequencies. So this indicates EAN has a higher apparent viscosity than water. This is also expected [32]. Secondly, the data points are not properly monotonically declining anymore. This happens to occur more often for EAN. Sometimes even at a higher immersion depth a better signal strength is measured. This should be an error, since more surrounded liquid means less measured signal. Thirdly, the exponential fit is left out. Since EAN is not Newtonian anymore the exponential model is not valid anymore. If the exponential fit is used even though a different value for the effective viscosity will be found. Since the powerlaw model consists of two parameters, n and K, another analytical model should be found. A relation between the amplitude of the signal and the immersion depth of the plate for a powerlaw fluid is given in (4.5) [3].

$$B(z) = (B_0^{1-n} + 2(1-n)\alpha_n(z - z_0))^{\frac{1}{1-n}} \tag{4.5}$$

Here $B(z)$ is the amplitude in V (which depends on immersion depth z), B_0 is the

initial signal strength at $z = 0$. n is the flow index parameter and α_n is given by (4.6).

$$\alpha_n = -\frac{1}{2d} 2\sqrt{2} P_3(n) \left(\frac{2\omega^n \rho_f^n K_n^{2-n}}{\rho_s G}\right)^{\frac{1}{2}} \tag{4.6}$$

Here d is the width of the plate in m, K is the other parameter named consistency and $P_3(n)$ is defined as (4.7).

$$P_3(n) \equiv -0.00630863n^3 + 0.0399466n^2 - 0.129211n + 0.448619 \tag{4.7}$$

4.2.1 Approach 1: Limit $dz \to 0$

Since this model has one more parameter to fit there is a reason to find out if this more complex model falls back to the Newtonian model for very small differences in immersion depth. So (4.5) is compared to the exponential solution of (4.8) if $z = z_0 + dz$, with dz very small:

$$E(z) = E_0 e^{-\alpha(z - z_0)} \tag{4.8}$$

Therefore both equations are Taylor expanded around z_0 following (4.9) (for the Newtonian model the amplitude B's are replaced by E's).

$$B(z_0 + dz) \approx B(z_0) + \frac{\mathrm{d}B}{\mathrm{d}z} \,|_{z_0}\, dz \tag{4.9}$$

Evaluating this expansion for both models gives (4.10) and (4.11).

$$B(z_0 + dz) \approx B(z_0) + \alpha_n B(z_0)^n \quad (Power - law) \tag{4.10}$$

$$E(z_0 + dz) \approx E(z_0) - \alpha_n E(z_0) \quad (Newtonian) \tag{4.11}$$

Both equations look quite similar. The sign is a matter of convention. In the Newtonian model α is defined positive, while for the powerlaw model a negative α is used. The only actual difference is the additional power of n at the right side of (4.10). So for $n = 1$ both formulas are equivalent. This seems logical since $n = 1$ gives the Newtonian model. Despite that for values of n that does not equal 1 the assumption is not valid anymore. This means the exponent can not be used for powerlaw liquids for small steps in z.

In short (4.5) has to be used to model the attenuation of a powerlaw liquid. Instead of one parameter both K and n should be investigated. This makes it a lot harder since both parameters has to be determined very accurate according to the model from (4.5). Small differences in n for example will result in very large differences in $B(z)$. Smith et al[4] already did some research on the rheology of EAN. A relation was found between the shear rate and the viscosity. A digitized version (using WebPlotDesigner)of this finding is shown in 18. Moreover a fit of the model in (4.12) is plotted to find the best corresponding values for the parameters K and n.

$$\tau_{xy} = -K(\frac{\mathrm{d}v_y}{\mathrm{d}x})^n \tag{4.12}$$

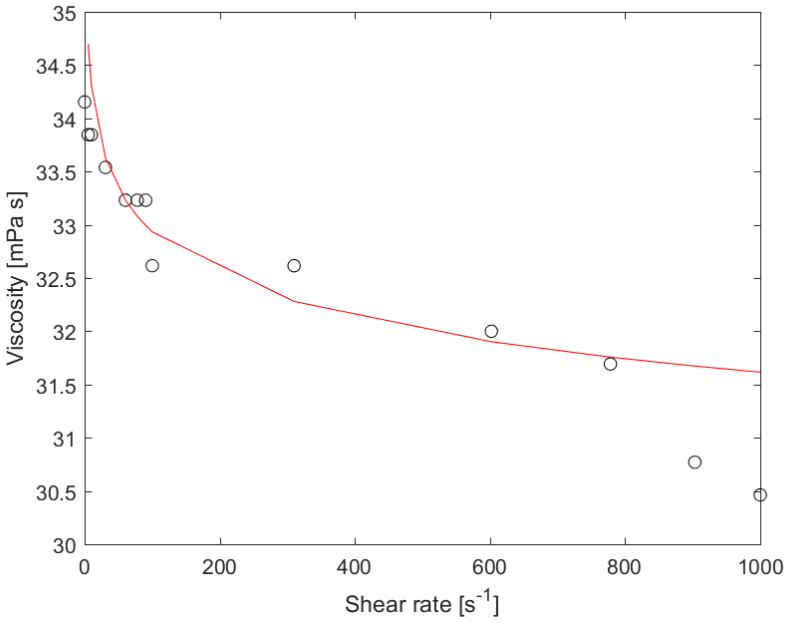

Figure 18: A digitalized plot of the literature data of Smith et al[4], including a red line which represents the model of (4.12). The fitted values are $K = 35.47 \pm 1.05 Ns^n m^{-2}$ and $n = 0.9822 \pm 0.006$

By looking at the graph the viscosity is not constant. It drops if the shear rate becomes larger, although very slowly. There is an uncertainty in the position of the points. This is due to the fact that the points had to be digitized. However the red line gives the following values for n and K, $n = 0.9822 \pm 0.006$ and $K = 35.47 \pm 1.05 Ns^n m^{-2}$. However by extrapolate K from the Smith et al graph the value becomes $K = 34.0957 Ns^n m^{-2}$, filling in $n = 0$ reduces the equation (4.12) to K. Remarkable is the difference in their uncertainties. This means the value of K can be determined quite precisely by the literature plot. On the contrary, n is more sensitive to errors. Suppose $n_1 = 0.99$ and $n_2 = 0.98$. For n_1 the power in (4.5) becomes 100 while for n_2 it is 50. So a very small difference in n would result into a very large error in the amplitude of the signal. For this reason it is not useful to built on these determined values for EAN. This means another method to look at the behaviour of EAN should be investigated.

4.2.2 Approach 2: Ratio's

This method is based on the ratio between different measured signal strengths to investigate on the rheological behaviour of a fluid. Because the relation between the viscosity of EAN and the frequency is unknown a possible alternative is to look at a fixed depth for different values of the frequency. If one examines the ratio between those frequencies the only parameter is α since z is fixed. The value for α can be determined for both Newtonian and power law liquids. Now the ratio could be a useful measure in comparing the rheological behaviour of these two types of fluids, because

both function in the denominator and numerator should be the same for one type of liquid at different frequencies.

First the analytical solution for the Newtonian model is calculated. For the derivation two decaying exponentials are used, namely $v_1 e^{-\alpha_1 z}$ and $v_2 e^{-\alpha_2 z}$. (z has no subscript since they are equal) The ratio P is determined in (4.13).

$$P = \frac{v_1 e^{-\alpha_1 z}}{v_2 e^{-\alpha_2 z}} = \frac{v_1}{v_2} e^{-(\alpha_1 - \alpha_2) z} \tag{4.13}$$

This could be rewritten into (4.14).

$$P = \phi e^{-\frac{z}{2h}(\frac{\eta \rho_f}{\rho_s G})^{\frac{1}{2}}[\omega_1^{\frac{1}{2}} - \omega_2^{\frac{1}{2}}]} = \phi e^{c[\omega_{ref}^{\frac{1}{2}} - \omega^{\frac{1}{2}}]} \tag{4.14}$$

Here $\phi = \frac{v_1}{v_2}$ (in theory v_1 should be equal to v_2 because they both indicate the initial amplitude of the signal, which should be the same at each measured frequency), ω_{ref} or ω_1 is a chosen reference frequency and ω_2 or ω, which is bigger than ω_{ref}, is a changeable frequency. Furthermore, c is defined as $c = \frac{z}{2h}(\frac{\eta \rho_f}{\rho_s G})^{1/2}$. This means if $\omega = \omega_{ref}$ the ratio $P = \phi = \frac{v_1}{v_2}$. For higher values of ω the ratio is also given by an exponent for a Newtonian liquid. The used η in (4.14) is based on the measured values at these depths (the viscosity is determined at $z = 0, 12.5, 25.0, 37.5$ and $50.0\ mm$). The values for the viscosity are determined by the ratio between the signal strength at a certain depth and the strength of the measured data point before (using (2.22)).

In figure 19 the ratio curves of water for different frequencies at four immersion depths are shown. Each data point is calculated by dividing the signal strength at the indicated frequency by the signal strength of the reference frequency, all for a fixed depth. For this graph the reference frequency is $3.0 MHz$ and the ratio is multiplied by $\frac{1}{\phi} = \frac{v_2}{v_1}$ to normalize the curve. The values for v_1 and v_2 are the coefficients a from (3.2) for the concerned frequencies. The uncertainties as well as the expected exponential fit functions are also added into the diagram.

By looking at figure 19 one should see that most data points agree with the fitted exponentials. As expected the graph of the smallest immersion depth would be on top and the graph with the biggest immersion depth at the bottom, since the latter attenuates the most. The uncertainties are based on the errors of coefficient ϕ, calculated by the uncertainties of v_1 and v_2. These are determined by the fit in MATLAB (error in fit parameter a). The errorbars are also based on the errors of ω and the uncertainty of the coefficient C. The formula to calculate the latter is given in (4.15).

$$\epsilon(C) = \sqrt{\epsilon(z)^2 + \epsilon(d)^2 + 0.5\epsilon(\rho_f)^2 + 0.5\epsilon(\rho_s)^2 + 0.5\epsilon(G)^2 + 0.5\epsilon(\eta)^2} \tag{4.15}$$

Here the error of C $\epsilon(C) = \frac{\sigma(C)}{C}$ and the error of z is determined by the concerned deviation, which is $0.1 mm$. The final equation for the error of the ratio P is given in (4.16) [29].

$$\frac{\epsilon(P)}{P} = \sqrt{(\frac{\epsilon(\phi)}{\phi})^2 + (\omega\epsilon(C))^2 + (C\epsilon(\omega))^2} \tag{4.16}$$

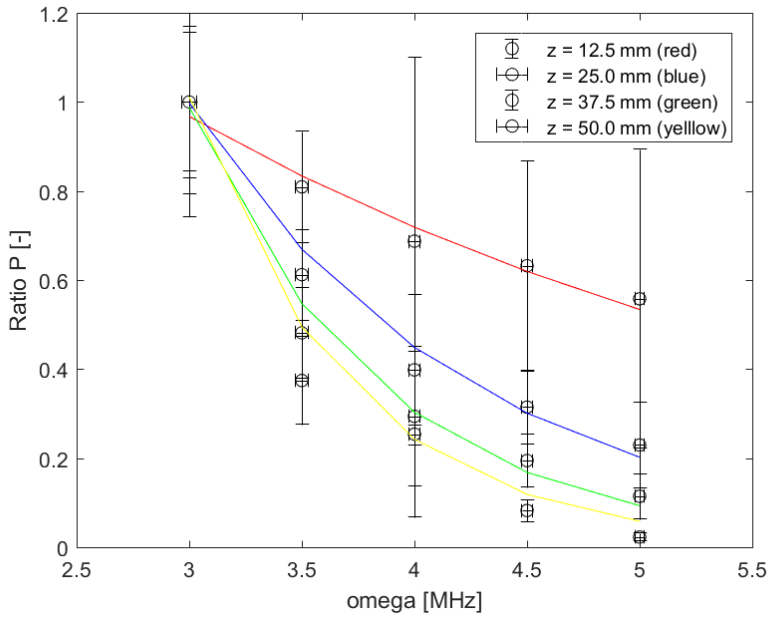

Figure 19: The ratio of the attenuation of water between different frequencies for fixed immersion depths including errorbars. The reference frequency is 3.0 MHz. The coloured lines are the fitted exponentials, following ae^{bx}. The uncertainties in a and b are given in table 3.

This formula is gained by some special error propagation. The whole deviation of (4.16) is given in Appendix C [29].

By looking at the uncertainties in figure 19 one should expect the smallest error of the ratio to be at the peak frequency around $3.7MHz$ [21], since signal should be the strongest compared to the included noise. However this effect is not clear in the figure. This can be caused by inaccurate measurements with an infected plate or disturbances, such as small movements of the components of the set up, during the experiment. Another source could be the fact that often the wave had to be regenerated because of an error message in the LABVIEW program. The new wave pulse could of course differ a little from the initial pulse, in phase for example. The errorbars are also relatively large. This could again be caused by the already 'contaminated' plate.

The uncertainty in the fitted parameters of the exponentials are given in table 3.

Table 3: Fitted parameters of the ratio graph 19, using ae^{bz} with their uncertainties.

$z[mm]$	12.5	25.0	37.5	50.0
a	2.361 ± 0.924	10.97 ± 6.29	34.25 ± 21.54	73.77 ± 73.03
b	-0.02974 ± 0.1036	-0.7992 ± 0.1685	-1.182 ± 0.1943	-1.43 ± 0.312

A promising thing is that for calculating a ratio no typical function, such as an exponential for Newtonian fluids, is needed (see (4.17)). This means that the ratio is given by the signal strength at the frequency of interest divided by the signal strength at the reference frequency. The signal strength depends on the fixed immersion depth, the rheology and the frequency. By normalizing this fraction of signal strengths the ratio between the searched functions is obtained, see (4.17).

$$P = \frac{v_1}{v_2}\frac{S(z_2, rheology, \omega)}{S(z_1, rheology, \omega)} = \frac{f(z_2, rheology, \omega)}{f(z_1, rheology, \omega)} \tag{4.17}$$

Here $\frac{v_1}{v_2}$ is the normalizing factor. Since both functions f have the same form, because the measurement is done with the same fluid and same immersion depth, a similar graph as for water can be made. This graph is illustrated in figure 20.

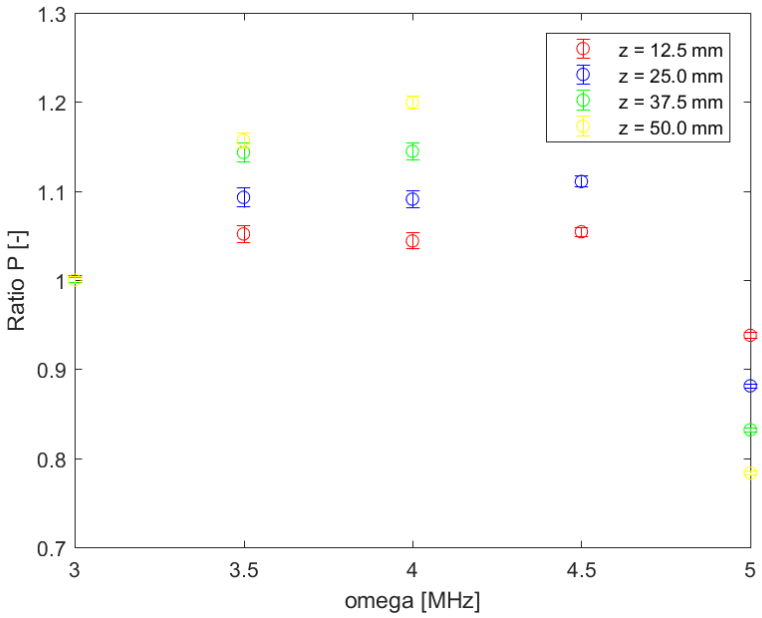

Figure 20: The ratio of the attenuation of EAN between different frequencies for fixed immersion depths including errorbars. The reference frequency is 3.0 MHz.

By looking at the curves in figure 20 the datapoints are oriented very differently compared to water. Some remarkable things could be noticed. Firstly, the trend of the graphs look a bit parabolic. This is logical, since for the peak frequency around $3.7MHz$ the signal strength compared with the included uncertainty should be larger than for other frequencies. Another thing to notice is the fact that for the frequencies 3.5, 4.0 and 4.5 MHz the ratio increases if the depth increases. This indicates that the effect of being attenuated becomes the best visible around the peak frequency. For 5.0 MHz the order is reversed. This is not correct. This and other possible errors could be causes by some things. A possible reason could be the fact that the plate in the small container often sticked against the walls of the container. Because of the smaller container the plate was only a few millimetres away from the sides and the tension of the fluid ensures the plate to stick to the container. Besides that, the amount of fluid inside the container varies a lot, because the fluid sticks onto the plate for instance. Secondly, the model is left out in this graph. An important thing is that v_1 and v_2 now are not obtained by the fitted parameter a from the exponential, but by the signal strength without the plate immersed into the fluid instead. So an extra measurement at $z = 0$ for all frequencies has too be done. Finally the uncertainty in the graph. Here the error of the ratio is determined by (4.2), using the RMS values in MATLAB.

In the next section the conclusions of this research are drawn.

Chapter 5: Conclusion

In this research the goal was to investigate on the viscosity determination of non-Newtonian fluids for the MSR. A number of interesting findings have been made. Using an ultrasonic waveguide and shear waves gave a lot of advantages to investigate on the attenuation caused by the fluid. In the introduction some research questions were introduced. Regarding these questions some conclusions could be made.

First of all, the waveguide method was used to determine the viscosity of water, which is a Newtonian fluid. Around the peak frequency at $4.0MHz$ a value of 1.4419 ± 0.0883 $mPas$ was found. Although all values lie above the literature value of 1.0526 $mPas$ at $18°$ C[31]. A major disturbance of the measurements on water was the fact that the plate is not cleaned after each measurement. So therefore the plate was still infected with a small layer of water. This affects the next measurement significantly. Therefore the calculated values for the viscosity are higher than expected.

The main interest was looking at a non-Newtonian fluid, because the used salts in the reactor are non-Newtonian too. The type investigated during this research is the powerlaw fluid named EAN. For EAN the signal clearly attenuates faster than for water, so this implies it has a higher viscosity than water. However a simple exponential model does not hold anymore. Because a power law fluid model consists of two parameter n and K. Using Smith at all the values for n and K were found, resulting in $K = 35.47 \pm 1.05 Ns^n m^{-2}$ and $n = 0.9822 \pm 0.006$. The value for K is quite well determined and reliable, however despite the small error for n it is not useful. The matter is that for a very small change in n the amplitude in the model will change significantly. Also for very small changes in the immersion depth one can not fall back on the exponential model, since an extra power of n appears in this limit case. So another method, where the ratio of the signal strength at a fixed immersion depth was measured, has been investigated.

For Newtonian fluids the ratio will also follow an exponential. This is clearly found by the measurements. The higher the depth, the stronger the attenuation of the ratio. For EAN the ratio between the signal strengths is normalized and the data points showed a parabolic trend, the peak is located approximately at the peak frequency of the transducer.

The measurements on EAN were plagued by a number of errors. Some automatic shutdowns of the LABVIEW program forces to set up a new wave pulse multiple times during a measurement. Besides that during the experiment a lot of fluid sticked to the plate. This made sure the amount of liquid and the level was not constant. At last for the small container the plate also sticked against the faces of the container and does not hang freely inside the container. All these things, including some small disturbances and changes in the set up, had a strong impact on the measurements.

5.1 Further research recommendations

In order to get a better insight in the behaviour of non-Newtonian liquids, EAN in this case, some subjects are useful to elaborate on:

- A larger container should be used to avoid sticking against the sides of the container. Another advantage is that the error of changing level of the fluid is smaller, since the sticked liquid picked up by the plate is percentage less.
- A longer plate should be used in order to measure a wider range of immersion depths. This gives more inside in the attenuation of EAN, since now only the very first part of the attenuation is measured.
- One should investigate on a rheological model for EAN. This gives the opportunity to know how the fluid behaves for different shear rates. Then also a accurate value for K and n could be found . If a method could be found how the τ_0 can be filtered from the measurements one can determine the rheology.
- More research should be done on the temperature dependency for EAN. By looking at the viscosity also a wider range of frequencies should be investigated to get a better view on the small decrease in viscosity for a higher shear rate.
- It is also useful to get into the transmission of the signal from the transducer into the plate, since this strongly affects the attenuation of the wave.

References

[1] Frédéric Bert Cegla. *Ultrasonic waveguide sensors for fluid characterisation and remote sensing.* Imperial College London, PhD Thesis, 2006.

[2] De Haas D. Verschuur E.D.J. Rohde M. Mastromarino S., Rook R. and Kloosterman J.L. *An Ultrasonic Shear Wave Viscometer for low viscosity liquids.* To be submitted.

[3] Rohde M. Internal report.

[4] Warr G.G. Smith J.A., Webber G.B. and Atkin R. *Rheology of Protic Ionic Liquids and Their Mixtures.* The journal of physical chemistry, University of Newcastle, Callagan, University of Sydney, Australia, Vol 8, 2013.

[5] Enerdata. Global energy statistical yearbook 2020.

[6] S. Blumsack R. B. Alley, D. Bice. Global energy sources.

[7] C. de la Vaissière et all. Generation i reactors.

[8] World Nuclear Association. Generation iv nuclear reactors.

[9] World Nuclear Association. Molten salt reactors.

[10] S. Surampalli. Is thorium the fuel of the future to revitalize nuclear?

[11] Wolfson R. *Essential University Physics Volume 2 (3rd).* Pearson, Boston, 2016.

[12] Rose J.L. *Ultrasonic Guided Waves in Solid Media.* Cambridge University Press, The Pennsylvania State University, 2014.

[13] J.S. Lowe Vogt T.K. and Cawley P. *Measurement of the material properties of vis-cous liquids using ultrasonic guided waves.* IEEE transactions on ultrasonics, ferroelectrics, and frequency control, Vol 51, No 6, June 2004.

[14] Challis R.E. Rabani A. and Pinfield V. *The torsional Waveguide Viscosity Probe: Design and Anomalous Behavior.* IEEE transactions on ultrasonics, ferroelectrics, and frequency control, Vol 58 No 8, August 2011.

[15] Challis R.E. Rabani A. and Pinfield V.J. *Rate of shear of an ultrasonic oscillating rod viscosity probe.* Elsevier Ultrasonics, University of Nottingham, February 2015.

[16] Sliteris R. Kazys R., Mazeika L. and Raisutis R. *Measurement of viscosity of highly viscous non-Newtonian fluids by means of ultrasonic guided waves.* Elsevier Ultrasonics, Vol 54, No 6, August 2014.

[17] Collins D. Mechanical properties of materials: Stress and strain.

[18] ResearchGate. Cauchy stress tensor for infinitesimal cube.

[19] Lai W.M and Krempl L. Cauchy stress tensor.

[20] Continuum mechanics. Divergence theorem.

[21] Rook R. *Viscosity determination of Newtonian fluids using shear ultrasonic guided wave attenuation.* Delft University of Technology, March 2020.

[22] Elmore W.C. and Heald M.A. *Physics of Waves.* Dover Publications, Swartmore College, Department of Physics, 1969.

[23] ResearchGate. Hooke's law and stress-strain curve.

[24] ResearchGate. Depiction of rayleigh wave showing elliptic particle motion.

[25] Schuringa O. *Density and viscosity calculation usingultrasonic wave propagation.* Delft University of Technology, December 2017.

[26] Van den Akker H. and Mudde R.F. *Transport Phenomena: The art of balancing.* Delft Academic Press, 2014.

[27] ResearchGate. Representations of apparent material viscosity.

[28] Carlroth. Safety data sheet.

[29] Hughes I.G. and Hase T.P.A. *Measurements and their uncertainties, A practical guide to mordn error analysis.* Oxford University Press, 2010.

[30] DBB. Saturated liquid density.

[31] IAPWS 2008 (Anton Paar). Viscosity of water.

[32] Wikipedia. Ethylammonium nitrate.

Appendix A: Determination attenuation coefficient for Newtonian fluids[3]

In this section a derivation of (2.18) is provided by using a balance over a small volume of the plate between z and $z + dz$. This balance is based on the power inside this volume element. First of all the dimensions of a small volume element of the plate are given in figure 21.

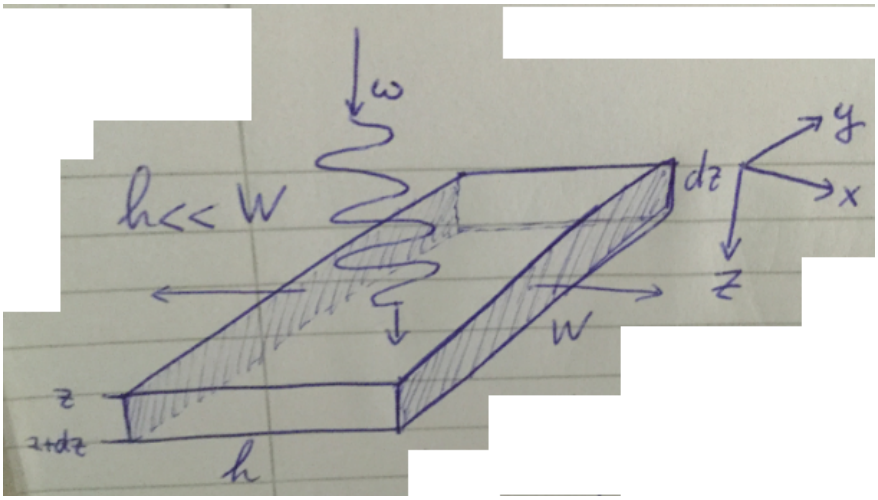

Figure 21: The dimensions used for the balance in the derivation of α for Newtonian fluids.

To simplify the calculation the plate is assumed to be very thin. This causes the loose of power at the sides of the plate to be negligible because $h << W$. So the shaded faces are the only parts that contribute to the balance. Furthermore the balance is assumed to exist under steady state conditions. In (A.1) the balance is given.

$$P_z(z,t) - P_{z+dz}(z,t) - 2\tau_0(z,t)v_0(z,t)W dz = 0 \tag{A.1}$$

Here P_z is the incoming power at $z = z$ and $P_z + dz$ is the outgoing power at $z = z + dz$. The losses at the two side faces give a negative contribution of both $-\tau_0 v_0 A$, where $A = W dz$. By taking dz very small the equation simplifies to a differential equation, see (A.2) and (A.3).

$$\frac{P_z(z,t) - P_{z+dz}(z,t)}{dz} = -2\tau_0(z,t)v_0(z,t)W \tag{A.2}$$

$$\frac{\mathrm{d}P_z}{\mathrm{d}z} = -2\tau_0 v_0 W \tag{A.3}$$

Because the plate does not move as a whole, but first the upper volume layer, than the layer below and so on. Therefore the power is averaged over a period $T = 2\pi/\omega$. This will result in the following integral in (A.4) and (A.5).

$$\frac{1}{T}\int_0^T \frac{\mathrm{d}P_z}{\mathrm{d}z} dt = \frac{\mathrm{d}}{\mathrm{d}z}\frac{1}{T}\int_0^T P_z dt = \frac{\mathrm{d}\tilde{P}_z(z)}{\mathrm{d}z} \tag{A.4}$$

$$\frac{\mathrm{d}\tilde{P}_z(z)}{\mathrm{d}z} = \frac{-2W}{T}\int_0^T \tau_0 v_0 dt \tag{A.5}$$

In order to analyze the integral the velocity as well as the shear stress should be known. The velocity of the wave is a function of x, z and t and is given by (A.6).

$$v(x,z,t) = B(z)e^{\frac{x}{\sqrt{2\nu}}}cos(kz-\omega t+x\sqrt{\frac{\omega}{2\nu}}) \tag{A.6}$$

Here B(z) is the amplitude of the wave at a certain value of z and $\nu = \eta/\rho_f$ is the kinematic viscosity. At $x = 0$ the equation becomes (A.7).

$$v_0(z,t) = B(z)cos(kz-\omega t) \tag{A.7}$$

The shear stress for Newtonian fluids is given by (A.8) [26].

$$\tau_{xy} = -\eta\frac{\mathrm{d}v_x}{\mathrm{d}y} \tag{A.8}$$

Combining (A.7) and (A.8) gives the shear stress at $x = 0$, see (A.9), which only depends on z and t. Here $\nu = \frac{\eta}{\rho_f}$ is used.

$$\tau_0(z,t) = -\sqrt{\frac{\eta B^2(z)\omega\rho_f}{2}}(cos(kz-\omega t)+sin(kz-\omega t)) \tag{A.9}$$

Rewriting (A.9) using the sum formulas gives (A.10).

$$\tau_0(z,t) = -(\eta B^2(z)\omega\rho_f)^{1/2}sin(kz-\omega t-\frac{\pi}{4}) \tag{A.10}$$

Now (A.5) is filled using (A.10) and (A.7), which results in (A.11)

$$\frac{\mathrm{d}\tilde{P}_z(z)}{\mathrm{d}z} = \frac{-2W}{T}B^2(z)(\eta\rho_f\omega)^{1/2}\int_0^T sin(kz-\omega t-\frac{\pi}{4})cos(kz-\omega t)dt \tag{A.11}$$

For evaluating the integral (A.11) the integrant is rewritten using Simpson's formulas and the double angle formula [3], see (A.12)

$$\frac{\mathrm{d}\tilde{P}_z(z)}{\mathrm{d}z} = \frac{-2W}{T}B^2(z)(\eta\rho_f\omega)^{1/2}\int_0^T(-\frac{\sqrt{2}}{4}+\frac{1}{4}sin(kz-\omega t-\frac{\pi}{4})cos(kz-\omega t-\frac{\pi}{4}))dt \tag{A.12}$$

Evaluating the integral and using the periodicity over 2π of the sinus the equation becomes independent of time. So the sinus as well as the period of the wave cancel out. In (A.13) the final result is displayed.

$$\frac{\mathrm{d}\tilde{P}_z(z)}{\mathrm{d}z} = -\frac{W}{2}(2\eta\rho_f\omega)^{1/2}B^2(z) \tag{A.13}$$

In [3] a formula is derived where the amplitude can be rewritten into the average power. The formula is given in (A.14).

$$\tilde{P}_z(z) = \frac{1}{2}\rho_s h W c(B(z))^2 \tag{A.14}$$

Combining (A.13), (A.14) (in a rewritten form) and $c = (\frac{G}{\rho_s})^{1/2}$ the differential equation could be rewritten into (A.15).

$$\frac{\mathrm{d}\tilde{P}_z(z)}{\mathrm{d}z} = -\frac{1}{h}(\frac{2\eta\rho_f\omega}{\rho_s G})^{1/2}\tilde{P}_z(z) \tag{A.15}$$

The solution of this differential equation is given by (A.16)

$$\tilde{P}_z(z) = P_0 e^{-2\alpha z} \tag{A.16}$$

where α is given by (A.17)

$$\alpha = -\frac{1}{2h}(\frac{2\eta\rho_f\omega}{\rho_s G})^{1/2} \tag{A.17}$$

For (A.16) holds that the factor 2 in the exponent is caused by the fact that power is proportional to the amplitude squared. By taking the derivative the extra factor is added.

Appendix B: Measurements on water and EAN

B.1 Water

Table 4: The measurements on water, the amplitude and attenuation are the coefficients in ae^{bz}. The viscosities at certain depths are determined by (2.22), using the concerned depth and the measurement before. The $\sigma(\eta)$ is calculated using (3.2). The units of α and η are $[Np/m]$ and $[mPas]$, as well as the corresponding errors (in this table the first measurement is taken into account).

ω $[MHz]$	amplitude a or v_n	attenuation b or α	$\sigma(a)$	$\sigma(b)$	$\eta(z = 12.5)$	$\eta(z = 25.0)$	$\eta(z = 37.5)$	$\eta(z = 50.0)$
3.0	1.5174	−1.5576	0.0409	0.0263	1.4811	1.5492	1.2479	1.7005
3.0	1.3854	−1.4725	0.1003	0.0707	1.1392	1.2945	1.3857	1.9648
3.0	1.4961	−1.5491	0.0856	0.0559	1.2396	1.5150	1.3853	1.6501
3.5	1.9978	−1.6270	0.0941	0.0460	1.3557	2.0056	1.9855	1.9427
3.5	1.9794	−1.6178	0.1047	0.0517	1.5033	1.9015	1.9801	1.7099
3.5	1.9504	−1.6033	0.1224	0.0613	1.4296	1.8661	1.7250	2.1279
4.0	2.5910	−1.5918	0.5105	0.1923	1.1638	1.4520	1.3759	1.0611
4.0	2.5509	−1.5735	0.4919	0.1882	1.0011	2.0367	1.5356	0.8859
4.0	2.6677	−1.6142	0.5803	0.2124	1.4469	1.9563	1.3708	1.0732
4.5	2.0829	−1.7598	0.0907	0.0425	0.9984	1.2614	1.3083	1.6160
4.5	2.0826	−1.7604	0.2725	0.1279	0.8570	1.2907	1.0061	–
4.5	1.9689	−1.7042	0.1427	0.0708	0.7067	1.5206	1.3138	1.5504
5.0	1.0800	−1.8922	0.1278	0.1158	0.8503	1.4027	1.9248	2.5382
5.0	0.9924	−1.8043	0.0258	0.0253	1.0980	1.5410	0.9193	1.7928
5.0	1.0312	−1.8579	0.2272	0.2152	0.5266	0.9915	0.9523	2.1856

Table 5: The measurements on water, the signal strengths, attenuation, viscosity including error and the temperature. These values are used or determined by (2.22). The signal strength are the RMS values at $z = 0.0mm$ and $z = 50.0mm$.

ω $[MHz]$	RMS signal strength $S_1(z = 50.0)$ $[V]$	RMS signal strength $S_2(z = 0)$ $[V]$	α $[Np/m]$	η $[mPas]$	$\epsilon(\eta)$ $[mPas]$	T $[°C]$
3.0	0.2954	0.3192	-0.7735	1.5246	0.0420	18.1
3.0	0.2944	0.3164	-0.7194	1.3189	0.0992	18.1
3.0	0.2937	0.3167	-0.7533	1.4462	0.0762	18.2
3.5	0.3617	0.3916	-0.7938	1.6057	0.0618	18.2
3.5	0.3619	0.3913	-0.7811	1.5550	0.0686	18.3
3.5	0.3617	0.3910	-0.7782	1.5434	0.0804	18.3
4.0	0.4862	0.5208	-0.6881	0.9048	0.2429	17.7
4.0	0.4881	0.5225	-0.6799	0.8835	0.2405	17.7
4.0	0.4889	0.5234	-0.6821	0.8892	0.2643	17.7
4.5	0.3280	0.3575	-0.8629	1.2648	0.0542	17.7
4.5	0.3281	0.3572	-0.8515	1.2316	0.1476	17.7
4.5	0.3309	0.3572	-0.7645	0.9928	0.0866	17.8
5.0	0.1487	0.1612	-0.9648	1.4230	0.1246	–
5.0	0.1492	0.1632	-0.8928	1.2186	0.0373	17.8
5.0	0.1466	0.1632	-1.0707	1.7526	0.2330	17.8

B.2 EAN

Table 6: The measurements on EAN, the RMS signal strength at different immersion depths with the corresponding standard deviation, determined by (4.2). The units of all RMS values are V.

$\omega\ [MHz]$	RMS $z = 12.5$	$\sigma(z = 12.5)$	RMS $z = 25.0$	$\sigma(z = 25.0)$	RMS $z = 37.5$	$\sigma(z = 37.5)$	RMS $z = 50.0$	$\sigma(z = 50.0)$
3.0	1.5278	0.0048	1.4009	0.0045	1.2919	0.0038	1.1674	0.00325
3.0	1.3073	0.0034	1.2580	0.0044	1.2063	0.0030	1.1718	0.0038
3.0	1.2518	0.0052	1.2477	0.0039	1.2110	0.0032	1.1733	0.0035
3.5	1.8662	0.0104	1.8404	0.0115	1.8302	0.0114	1.7865	0.0085
3.5	1.9273	0.0094	1.9306	0.0100	1.9289	0.0106	1.7980	0.0083
3.5	1.8912	0.0090	1.8804	0.0109	1.8546	0.0101	1.7951	0.0084
4.0	2.0746	0.0083	2.0580	0.0097	2.0557	0.0122	2.0213	0.0065
4.0	2.0349	0.0093	2.0490	0.0099	2.0401	0.0081	2.0203	0.0076
4.0	2.0343	0.0089	2.0355	0.0084	2.0238	0.0093	2.0322	0.0073
4.5	1.7257	0.0059	1.7288	0.0070	1.7032	0.0078	1.7085	0.0052
4.5	1.6548	0.0057	1.6697	0.0058	1.6766	0.0065	1.7068	0.0057
4.5	1.5927	0.0033	1.6146	0.0054	1.6519	0.0074	1.7005	0.0065
5.0	1.6727	0.0029	1.5039	0.0024	1.3474	0.0036	1.2033	0.0021
5.0	1.6570	0.0029	1.4951	0.0021	1.3443	0.0020	1.1975	0.0022
5.0	1.7027	0.0030	1.5241	0.0024	1.3621	0.0018	1.2137	0.0022

Table 7: The measurements on EAN, the signal strengths, attenuation, viscosity including error and the temperature. These values are used or determined by (2.22). The signal strength are the RMS values at $z = 0.0mm$ and $z = 50.0mm$.

ω $[MHz]$	RMS signal strength $S_1(z = 50.0)$ $[V]$	RMS signal strength $S_2(z = 0)$ $[V]$	α $[Np/m]$	η $[mPas]$	$\epsilon(\eta)$ $[mPas]$	T $[°C]$
3.0	1.1674	1.7247	-3.9024	30.8616	0.1317	19.2
3.0	1.1718	1.3098	-1.1133	2.5119	0.2451	19.2
3.0	1.1733	1.2389	-0.5444	0.6006	1.0442	19.2
3.5	1.7865	1.8708	-0.4610	0.3690	0.5269	19.5
3.5	1.7980	1.9013	-0.5588	0.5423	2.0002	19.3
3.5	1.7951	1.8846	-0.4861	0.4105	0.8040	19.3
4.0	2.0213	2.1030	-0.3965	0.2390	0.9183	19.2
4.0	2.0203	2.0404	-0.0989	0.0149	2.0002	19.3
4.0	2.0322	2.0160	0.0799	0.0097	1.6763	19.4
4.5	1.7085	1.7319	-0.1357	0.0249	1.0242	19.2
4.5	1.7068	1.6294	0.4646	0.2916	0.3393	19.3
4.5	1.7005	1.5759	0.7606	0.7815	0.2642	19.6
5.0	1.2033	1.8343	-4.2158	21.6100	0.0532	19.3
5.0	1.1975	1.8730	-4.4731	24.3266	0.0530	19.5
5.0	1.2137	1.9077	-4.5225	24.8683	0.0351	19.3

Appendix C: Error propagation for the ratio P

For Newtonian fluids the ratio P could be calculated mathematically since the attenuation of the signal strength follows a decaying exponential. Therefore the ratio P also is an exponential function. The derivation is given in the results section. The ratio is shortly given in (C.1).

$$P = \phi e^{c\omega} \tag{C.1}$$

Here ϕ, c and ω all have a certain error. In order to determine the error of the ratio these have to be propagated according to the formula above. The error P is calculated using (C.2).

$$\epsilon(P) = P(\phi + \epsilon(\phi), c + \epsilon(c), \omega + \epsilon(\omega)) - P(\phi, c, \omega) \tag{C.2}$$

A Taylor expansion is used to elaborate on the first term, see (C.3).

$$P(\phi + \epsilon(\phi), c + \epsilon(c), \omega + \epsilon(\omega)) = P(\phi, c, \omega) + \frac{\mathrm{d}P}{\mathrm{d}\phi}\epsilon(\phi) + \frac{\mathrm{d}P}{\mathrm{d}c}\epsilon(c) + \frac{\mathrm{d}P}{\mathrm{d}\omega}\epsilon(\omega) \tag{C.3}$$

By filling in (C.3) in (C.2) the result becomes (C.4).

$$\epsilon(P) = \frac{\mathrm{d}P}{\mathrm{d}\phi}\epsilon(\phi) + \frac{\mathrm{d}P}{\mathrm{d}c}\epsilon(c) + \frac{\mathrm{d}P}{\mathrm{d}\omega}\epsilon(\omega) \tag{C.4}$$

Now the derivative can be obtained using (C.1). This comes down to (C.5).

$$\epsilon(P) = e^{c\omega}\epsilon(\phi) + \phi\omega e^{c\omega}\epsilon(c) + \phi c e^{c\omega}\epsilon(\omega) \tag{C.5}$$

This can be rewritten as (C.6).

$$\frac{\epsilon(P)}{P} = \frac{\epsilon(\phi)}{\phi} + \omega\epsilon(c) + c\epsilon(\omega) \tag{C.6}$$

Mostly the conventional way of writing the error is the quadratic formulation, which is given in (C.7) [29].

$$\frac{\epsilon(P)}{P} = \sqrt{(\frac{\epsilon(\phi)}{\phi})^2 + (\omega\epsilon(c))^2 + (c\epsilon(\omega))^2} \tag{C.7}$$